

**Cleaning Up Clean Energy: Sustainable End-of-Life Practices for Photovoltaics**

Team SOLAR

Riordan Correll-Brown, Ashley Didriksen, Vincent Du, Eric Fagan, Shannon Ganley,

Vikram Hanspal, Ryan Horvath, Steven Shockley, Christine Zhou

Gemstone Honors College

University of Maryland, College Park

Research conducted under the advisement of Dr. Bao Yang

Discussants: Dr. Raymond Adomaitis, Dr. Oded Rabin, Dr. Joe Sullivan,

and Dr. Kiran Raj Goud Burra

## Abstract

As the first generation of large-scale solar installations begins to reach the end of their 25-year lifespan and solar power becomes more prevalent, solar waste is becoming an increasingly pressing global issue. Solar panels are difficult to disassemble and often end up in landfills, where they leach toxic metal compounds into the environment after disposal. Solar panel recycling can help ameliorate these environmental impacts, but existing recycling techniques often employ harmful chemicals or thermal treatments, which produce undesirable byproducts. This project aims to address environmental concerns associated with ethylene vinyl acetate (EVA) removal, one of the most challenging aspects of solar cell recycling. EVA is an adhesive polymer that joins the glass, silicon solar cell, and backsheet layers together. In this work, we investigate the effect that five chemical alternatives to toluene have on EVA. Gasification and pyrolysis are also explored as an alternative to chemical dissolution methods. Mass loss data and qualitative observations of post-treatment indicate that the chosen solvents can effectively aid in panel disassembly, with some demonstrating results similar to toluene. This project identifies multiple solvents that are promising candidates for the chemical treatment of solar cells for recycling purposes, whose environmental impacts are lower than those currently used in industry. However, the findings also underscore the difficulty of developing a solar panel recycling process free from harmful chemical waste and demonstrate the need to design panels with recycling in mind, especially through the use of alternative encapsulant and backsheet materials.

## **Acknowledgments**

The members of Team SOLAR would like to give special thanks to the following individuals: Dr. Bao Yang, for guiding us through our project and serving as the team mentor; Dr. Xinan Liu and Dr. Gupta, for providing laboratory space; Ms. Jodi Coalter and Ms. Sarah Weiss for serving as the team librarians; Dr. Ingrid Repins, Dr. Mike Kempe, and Dr. John Magnum at the National Renewable Energy Laboratory, for their advice on our project direction; and Dr. David Lovell, Dr. Allison Lansverk, Dr. Kristan Skendall, Dr. Vickie Hill, Ms. Leslie Lizama, Jon Brodsky, and the remainder of the Gemstone staff. Finally, we would like to thank our discussants Dr. Raymond Adomaitis, Dr. Oded Rabin, Dr. Joe Sullivan, and Dr. Kiran Raj Goud Burra.

This report was prepared by Gemstone Team SOLAR under awards NA14OAR4170090 and NA18OAR4170070 from Maryland Sea Grant, National Oceanic and Atmospheric Administration, U.S. Department of Commerce. We would also like to thank the University of Maryland Sustainability Fund, Sigma Xi Undergraduate Research Grant, and the Do Good Institute for the delegation of funds from their grants.

The statements, findings, conclusions, and recommendations are those of the authors and do not necessarily reflect the views of Maryland Sea Grant, the National Oceanic and Atmospheric Administration, or the U.S. Department of Commerce. The Sustainability Mini-Grants are intended to provide funding to encourage the development or maintenance of projects or programs that improve the sustainability of the UMD campus and/or enhance opportunities for students to learn about sustainability issues.

## Table of Contents

<b>Abstract</b>	<b>2</b>
<b>Acknowledgments</b>	<b>3</b>
<b>Table of Contents</b>	<b>4</b>
<b>Introduction &amp; Background</b>	<b>5</b>
Solar Panel Varieties & Composition	7
Solar Panel Failure & Environmental Harm	10
Current Industrial Practices for Solar Panel Recycling	12
Thermal Treatments, Pyrolysis, and Gasification	16
Chemical Treatments and Solvent-Based Removal	18
Green Solvents and Criteria for Solvent Harm	19
Policies and Adoption	21
<b>Methodology</b>	<b>24</b>
Solvent Selection for Chemical Testing	24
Panel Disassembly and Sample Preparation	31
Solvent Testing Procedure	34
Gasification Procedure	34
<b>Results &amp; Discussion</b>	<b>38</b>
Solvent Testing	38
Gasification & Pyrolysis of EVA	52
<b>Conclusions and Future Works</b>	<b>57</b>
Conclusions	57
Contribution	57
Future Work	58
<b>Appendices</b>	<b>61</b>
<b>References</b>	<b>64</b>

## **Introduction & Background**

The elimination of greenhouse gasses from the atmosphere is a critical step in the fight against climate change. Fossil fuels still account for the majority of energy produced worldwide, but the renewable energy market has grown exponentially within the last few years (Aman et al., 2015). The solar energy sector, in particular, is growing quickly and is predicted to increase from 11% of the United States' renewable energy capacity in 2017 to 48% in 2050 (Tabassum et al., 2021). In 2017, the global power capacity of photovoltaic (PV) devices reached 400 GW and is projected to reach 4500 GW by 2050 (Chowdhury et al., 2020). With increasing installations, the number of solar panels completing their lifespan will increase. Consequently, PV waste will rise. In 2016, there were 250,000 tons of PV waste globally; this figure is projected to increase to 78 million tons by 2050 (IRENA, 2016). As our global use of solar energy increases, we need to ensure that we are prepared to handle PV waste and the environmental impact of PV end-of-life processes.

Though renewable energy sources produce significantly less carbon dioxide than coal and natural gas, the manufacturing, disposal, and recycling processes associated with these sources still have an environmental footprint. Solar power in particular poses a number of environmental risks when compared to other renewable energy sources. Over their life cycles, solar energy devices produced more greenhouse gasses on average than wind, nuclear, or hydroelectric energy devices, due to their significantly greater quantity of material components (Hou et al., 2016). Both the manufacturing and recycling processes of solar panels should be recognized as environmentally impactful, as the manufacturing byproducts and material components can be toxic. Their release into the environment, especially when panels are improperly disposed of, can

create environmental and human health hazards (Aman et al., 2015). There is a gap, both in scientific research and policy, in the handling of solar panel manufacturing and recycling that leaves ecosystems and communities vulnerable.

In the long term, everyone is affected by pollution and climate change. However, low-income communities often have less recourse to fight legal battles against companies practicing unsafe waste disposal methods in their area, and can be disproportionately impacted by the effects of climate change (Boyd et al., 2021). In addition, workers in manufacturing and waste management or recycling plants are directly impacted by the chemicals used to make and recycle PV technology. Electronic waste is a rising issue that disproportionately impacts low-income areas globally (Ogunseitan, 2023). Though photovoltaics are just one component of this problem, by improving the feasibility of solar recycling we can improve the overall lifecycle impact of solar technologies, both preventing these negative impacts and encouraging the further development of solar technologies over fossil fuel consumption. One of the fundamental aims of our research is to reduce the harmful effects of solar panel technologies in their EOL stages, and thereby reduce these harmful and disproportionate impacts.

It is critical to establish a safe, efficient, and reliable method for the disposal of solar panels now rather than later. Most solar panels have a life expectancy of 25-30 years, which means that we are approaching the first wave of solar panels that will be retired en masse (Contreras-Lisperguer et al., 2017). For this reason, we focused our research efforts on the recycling of crystalline silicon solar cells, as they are the most common type currently in use and will have the greatest demand for recyclability in the near future. Unless there is infrastructure in place to properly process and potentially re-use these panels, their waste, including silicon, tellurium, cadmium, and other heavy metals, has the potential to cause environmental

contamination, damaging ecosystems and their surrounding communities (Latunussa et al., 2016). The problem of proper solar panel recycling stems from both solar technologies themselves and the policies surrounding their disposal.

### *Solar Panel Varieties & Composition*

The wide breadth of research in the field of photovoltaics seeking to improve solar panel efficiency, ease of manufacturing, and expected lifetime, has given rise to a large variety of photovoltaic technologies (Dambhare et al., 2021). Despite this variety, there are a few underlying constants for whatever panel type is chosen— there is always an encapsulating material and a photoreactive material used to generate the charge from the light on the panel. There are several variants of solar panels currently on the market, and each varies heavily in composition, structure, and manufacturability. The primary focus of this research has been on mono and polycrystalline silicon photovoltaics, which pose the most urgent recycling challenge.

The traditional variant is silicon photovoltaic cells, which are the most common in use today, composing 90% of the panels on the market due to the ease of manufacturing and low cost (Abdo, 2023). The structure of the cells themselves is also variable, with both individual monocrystalline cell arrays and polycrystalline merged cells being present in separate models of solar panels (Dambhare et al., 2021). Monocrystalline cells are made by slowly forming silicon into a rod and then using the diamond wire method to slice the silicon into wafers, whereas polycrystalline cells are made by melting silicon into a large ingot before slicing; these methods result in differences in the crystal structure of the silicon layer in the solar panel (Jiang et al., 2020).

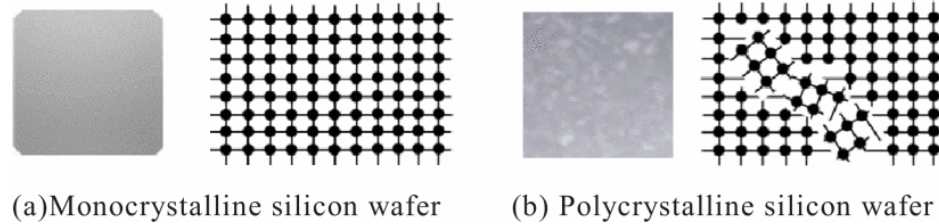


**Figure 1.** Crystalline structure of silicon layer in a solar panel (figure from Jiang et al., 2020).

These differences in the crystal structure of the silicon semiconductor layer result in (for the monocrystalline) greater efficiency, and (for the polycrystalline) cheaper production (Jiang et al., 2020). One study found the difference in efficiency to be 9.22% for the monocrystalline and 7.94% for the polycrystalline (Hidayanti, 2020). Both forms of the silicon solar panel are common throughout global installations, and, for our purposes, are identical in their recyclability.

These semiconductor modules are then surrounded with an encapsulant—most commonly ethylene-vinyl acetate (EVA)—in order to help protect the cells from external factors like physical or moisture damage when they are in the field. EVA is a copolymer of ethylene and vinyl acetate and functions as an adhesive and laminate in the panel. This polymer layer is cured by thermal treatment, commonly at 150°C, to allow cross-linking, increasing the strength of the adhesive layer which holds many of the panel components together (El Amrani et al., 2007). Afterward, a sheet of glass is applied to the front and a backsheet composed of variable materials is applied to the back of the panels for further protection against external damages; common materials for the backsheet include polyvinyl fluoride (PVF) (Geretschläger et al., 2016). A junction box is connected to the internal systems through the backsheet to help protect them from unexpected surges or issues with connection, and the panel itself is closed within a frame. This frame is usually aluminum but can vary based on make and model. Figure 2 below shows the

arrangement of the typical components of both a silicon-based panel and a Cadmium Telluride (CdTe) thin film, discussed further below.

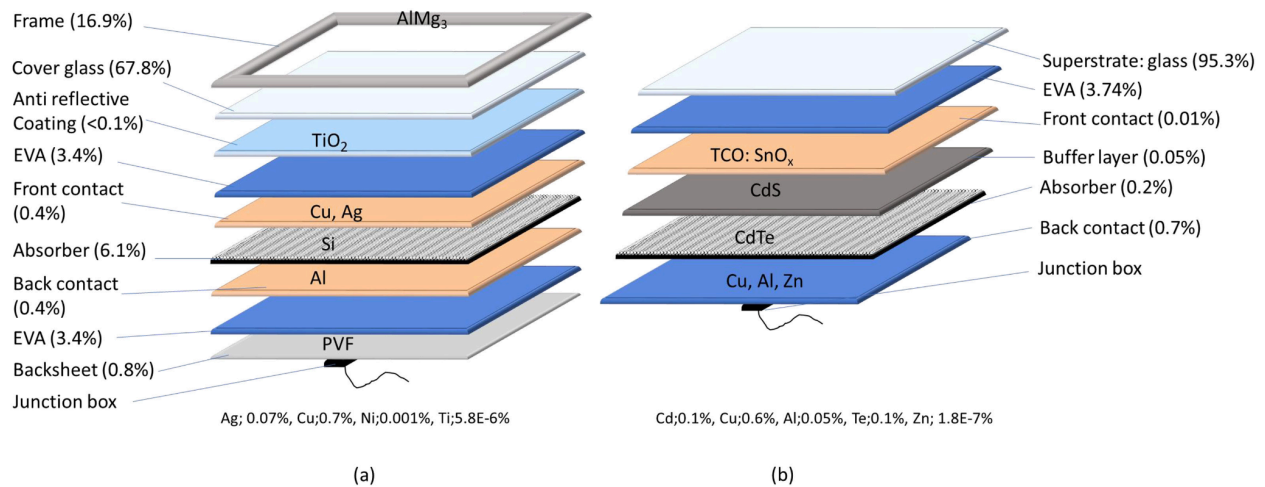


**Figure 2.** Components of a typical (a) silicon and (b) thin film solar panel with percent composition by weight (figure from Maani et al., 2023).

The second most common panel type in use is thin-films, which have substantially different compositions and designs than their predecessors. Notably, they lack the rigid structure of the frame and the thick glass sheets seen in early-generation solar panel designs. Because they lack this rigid superstructure, they are often more difficult to damage than their silicon counterparts (Maalouf, 2023). The major difference is the way that these films are created; thin films are formed by directly depositing the semiconductor material onto the flexible substrate layer, or adsorber, rather than by the formation of distinct “wafers” as in the silicon panels (Maalouf, 2023). A protective layer of encapsulants is added around the panels afterward, which is again commonly EVA (Dintcheva, 2023).

Though the traditional silicon-based and newer thin-films dominate the solar panel market, this is an active field of research, and there are countless other structures and materials

that are used in solar panels. Newer panels may have light-absorbent materials doped onto the panel to allow for greater electron absorption and conductivity, or they may have nanostructures of anti-reflectives built on the surface or etched into the panel to achieve greater overall efficiency (Dintcheva, 2023). The encapsulation materials can also vary widely based on the panels in question, as new techniques like vacuum lamination allow for a wider range of encapsulants to be feasibly used (Dintcheva, 2023). Silicon encapsulants have also been tested in panels, being baked on and exposed to ultraviolet light treatments to develop the structure of the encapsulant further (Dintcheva, 2023).

Though an overwhelming majority of commercial panels still consist of silicon or cadmium telluride, the types of semiconductors used in panels also continue to evolve. For example, thin-film gallium-arsenide cells are not only smaller than regular silicon cells but allow for exceptionally high efficiency rates of up to 29% with a single-junction cell (Maalouf, 2023). Multi-layer or multiple-junction cells can achieve even higher efficiencies, with some triple-junction cells managing to reach 37.9% efficiency and a 6-junction cell managing 39.6% (Papež, 2021). However, due to the high cost of manufacturing and relative rarity of the constituent materials, they are far less common and— due to their recent development— often far younger than other types of panels in use. In this study, we focus our efforts on the silicon solar panel, which has the most pressing need for adequate recycling capabilities in the near future.

### *Solar Panel Failure & Environmental Harm*

Solar panel efficiency degrades at a rate of about 0.5% every year (Skomedal et al. 2020). Silicon photovoltaics have several distinct failure mechanisms. The most common factor for panel failure is prolonged exposure to UV rays and inclement weather conditions, which

gradually degrades the encapsulant layer (Chowdhury et al., 2020). Another common failure point is damaged glass through human errors in the assembly or installation of the panels creating micro-cracks or scratches, speeding up their degradation (Chowdhury et al., 2020). Glass can also be broken by falling objects such as trees. Electrical problems such as those from wiring issues with junction boxes, fusebox damage, and charge controller failure can reduce the efficiency of solar arrays or cause total failure (Chowdhury et al., 2020).

Though solar power is a renewable energy source with a significantly lower environmental footprint than the burning of fossil fuels, environmental issues could arise from the mismanagement of end-of-life panels. Solar panels are composed of dangerous materials, including lead, cadmium, and arsenide. If not properly disposed of, these metals can leach into the environment, damaging ecosystems and—in large enough quantities—endangering human health (Xu et al., 2018). They can also enter nearby ground and surface water sources, causing harm to people. Previous studies have looked into the feasibility of this issue.

A 360-day-long laboratory experiment investigated the effects of broken solar panels in groundwater. Several 5x5 cm<sup>2</sup> solar panel fragments from various types of solar panels were submerged in water-based solutions of various pH levels, emulating groundwater environments. The results showed substantial leaching of metals, such as cadmium and lead, surpassing the World Health Organization's permissible limits for drinking water (Nover et al, 2017). Another case study of a hypothetical landfill with solar waste based on a model that pools together data from previous studies was estimated to have a leachate pollution index of 15.32 which greatly exceeds the recommendations by the Indian MSW Management and Handling Rules of 7.378. Leached metals include iron, copper, nickel, zinc, lead, chromium, and arsenic (Nain and Kumar, 2020). Heavy metals such as those pose a serious risk to human health including organ damage,

neurological defects, respiratory disorders, and carcinogenicity (Mitra et al., 2022). These results confirm that proper disposal of solar modules is necessary for the safety of people and our environment, especially given the disproportionate impact on vulnerable people (Cannon, 2020).

It is important to acknowledge the potential environmental impact associated with the manufacturing of solar panels, particularly in areas related to wastewater management and the use of harmful extraction of raw material from the earth. However, as this is a complex topic, it fell outside the scope of this study. We have chosen to focus solely on EOL recycling to reduce the lifecycle impacts of photovoltaic technologies, improving their overall sustainability and longevity as a renewable energy resource.

#### *Current Industrial Practices for Solar Panel Recycling*

Currently, the cost of recycling solar panels is much higher at \$15-\$45 per module than disposing of them in a landfill which costs \$1-\$5 (U.S. Dept of Energy Solar Energy Technologies Office, 2022). To provide an incentive to recycle modules, the cost must be reduced. This can be done by improving recycling techniques to reduce their inherent cost or increase the value of the recovered materials. This is an active field of research; some groups have reported as high as \$11-12/module in revenue from solar panel recycling, using methods such as sequential electrowinning to separate and extract multiple valuable/toxic metals from the PV module (Huang et al., 2017). While promising, this process requires the use of harmful chemicals and produces harmful byproducts, discussed further later. These chemical byproducts complicate the scalability of such a process to the industrial level; for this reason, most solar recycling processes currently in use rely heavily on mechanical methods that focus only on material separation, despite their lower returns in revenue. A life cycle analysis that compared

recycling methods for solar panels found that most chemical and mechanical techniques aimed at delamination of the solar panel ultimately have a greater life cycle impact (are worse for the environment) than simple material extraction since these methods are often developed in the lab and not optimized for the industrial scale (Maani et al., 2020).

Mechanical crushing is the dominant form of solar panel recycling currently used in the US; it is cheap and requires little new technology, but is not very productive for material recovery. This broad term can include many techniques but typically has the goal of material extraction—recovery of some high-value materials, like silicon and glass—not delamination, the recovery of *intact* high-value materials, like silicon wafers (Isherwood, 2022). Common steps in the mechanical crushing and material recovery process include panel disassembly (removal of the junction box, aluminum frame), use of a shredder, hammer mill machine, or both (to reduce panel sizing and overcome lamination), and a multitude of separatory techniques, such as particle sieving, flotation, chemical leaching, and thermal processes like pyrolysis (Isherwood, 2022). Each of these can be used to remove different panel components from the fine gravel mixture which remains after crushing, but the purity of these extracted components is typically low and, for example, not ready for reuse in solar panels, requiring additional chemical purification steps.

One process that has been proposed, dubbed the Double Green Panel process, involves the sequential processing of a solar panel through a shredder, hammer mill crushing, wet-mechanical treatments, and floating (Figure 3, Giacchetta et al., 2013). This process intentionally minimized the use of chemical and thermal treatments in favor of a diverse set of mechanical ones; life cycle analysis and economic feasibility analysis have been completed on this process, with promising results (Marchetti et al., 2018). The major drawback of this process, and others like it, is that the resulting extracted materials (largely glass and silicon) are not

purified, and therefore require additional purification steps, which are not included in this life cycle analysis study (Marchetti et al., 2018). These steps have the potential to be costly in terms of energy and time and often require the same chemical and thermal treatments this process aims to avoid.

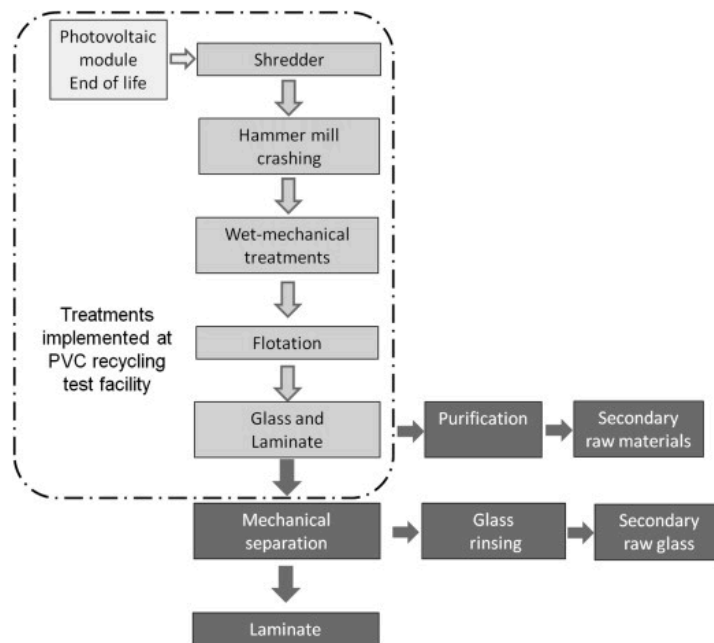


**Figure 3.** Double green panel recycling process (figure from Giacchetta et al., 2013).

Because of these impure products, panel crushing usually does not generate materials that can be salvaged for reuse in other panels or electronics. Instead, the waste is treated as scrap metal and can be used to, for example, reinforce concrete (Latunussa et al., 2016). Glass may be recoverable through this method, which is the most profitable output; other waste is mixed, and so has little value, making this method promising for businesses but not for complete material recovery (Granata et al., 2014). This means that the higher-value metals, including silicon, are lost or impure. Mechanical treatments also produce dust and noise pollution (Padoan et al., 2019).

The first industrial-scale recycling method for thin-films used in the United States was developed by First Solar; this process involves shredding, crushing in a hammer mill, and then chemical treatments using sulfuric acid and hydrogen peroxide to remove the EVA laminate (Giacchetta et al., 2013). Similar to other methods, this results in 90% recovery of the glass, and 90% recovery of the semiconductor materials—in this case, cadmium and telluride (First Solar 2017). Again, the main drawback of this method is the use of crushing, which improves the ease of materials separation but results in the need for further purification of glass and semiconductor materials before they can be reused.

In most mechanical crushing or hammering methods, thermal treatment is also utilized to degrade the cross-linked EVA layer; one study used a furnace at 650°C after crushing, finding that the purity of glass fragments recovered was greatly increased following thermal treatments, leading to greater recyclability (Granata et al., 2014). The recovery of pure fragments of rare metals and silicon (or other semiconductor materials in the case of thin films) from recycled solar panels is an ongoing challenge in the field. For this, we turn our focus from materials extraction to delamination, requiring more intensive thermal and chemical methods.

### *Thermal Treatments, Pyrolysis, and Gasification*

Many proposed methods for solar panel delamination require the use of thermal treatments, some as simple as heating to complement other mechanical and chemical methods, while others favor entirely thermal treatments, such as pyrolysis.

There are limited existing experiments using exclusively thermal treatments for recycling solar panels. One group performed pyrolysis of EVA polymer using thermogravimetric (TGA) and differential thermal analysis (DTA) (Zeng et al, 2004). They found three main endothermic

peaks, the first at 63° C which is the melting point of the EVA used. A second peak at 334°C reflects the endothermic degradation in the first pyrolysis stage. A third peak at 450°C reflects an exothermic peak (Zheng et al, 2004). This experiment performed the TGA and DTA analysis under different oxidizing atmospheres. When exploring the pyrolysis gas produced, they took averages over 20 experiments at various heating rates. On average, the product gas was 26.11% CO<sub>2</sub>, 22.12% CH<sub>4</sub>, and 8.43% H<sub>2</sub>, in terms of volumetric concentration, with the remainder being other hydrocarbons (Zheng et al, 2004). Of the 100 g of EVA undergoing pyrolysis: 10 g became gas, with 89.9 g becoming condensate and 0.1 g as a residue.

Gasification is another method of thermal treatment. The key difference between gasification and pyrolysis is the presence of oxygen. Pyrolysis happens without the presence of oxygen while gasification uses a controlled amount of oxygen (below what is necessary for combustion). Gasification is useful in that the main byproduct, syngas, can have useful applications such as being a fuel for power generation. Pyrolysis typically produces a liquid, char, and limited gas.

A group explored composing polyethylene glycol terephthalate (PET) and EVA using a unique vacuum-gasification-condensation setup. At 505°C and 10 Pa the PET and EVA underwent gasification (Qin et al., 2020). To obtain material for sampling, researchers crushed full solar cells into particles and used a screening mesh to separate the EVA and PET. Their results of the TGA and the derivative thermogravimetric analysis (DTG) are shown below in Figure 4.

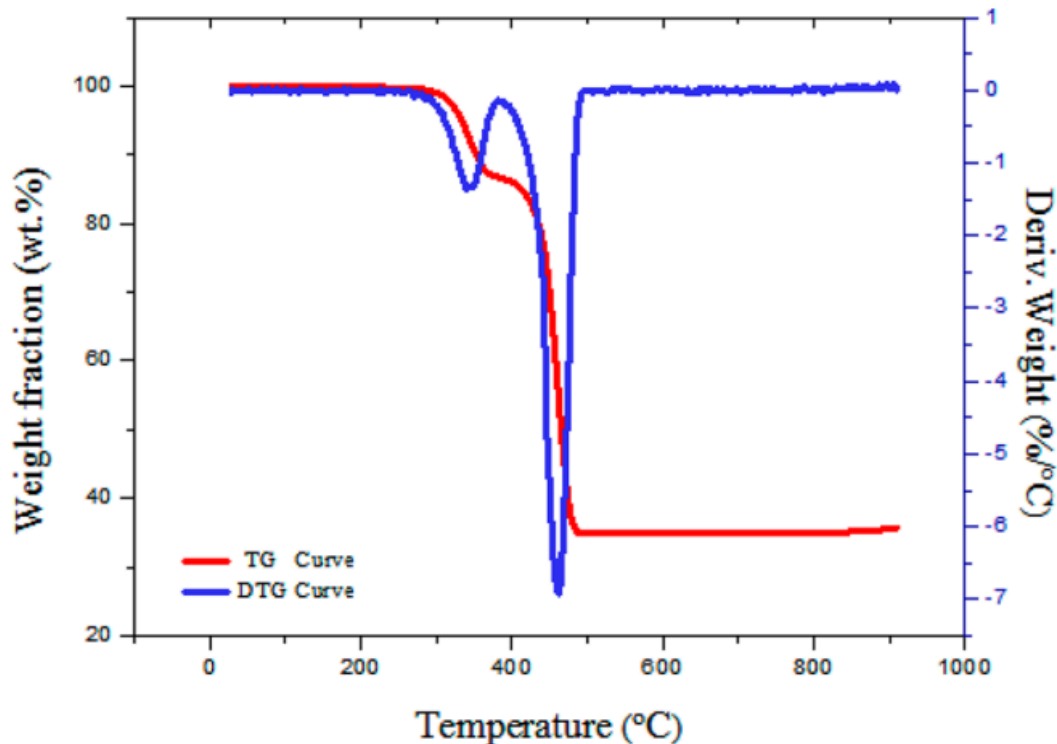


**Figure 4.** DTG and TG curves of mixed PET and EVA (figure from Qin et al., 2020).

From their TGA analysis, it is found that from 297 to 490°C, the PET/EVA completely decomposes and above 490°C the weight does not change, i.e. it is completely decomposed (Qin et al., 2020). The fastest mass loss was at 461°C which indicates the organics components “decomposed violently” (Qin et al., 2020). This study analyzes the condensation oils and residue left from their gasification-condensation set-up however, they do not review the syngas development.

In reviewing these existing thermal treatment experiments of EVA, it is clear there is a gap when evaluating the viability of gasification and the potential usefulness of the syngas. As explored in the methodology, gasification experiments of EVA are explored with TGA analysis and a review of the syngas developed.

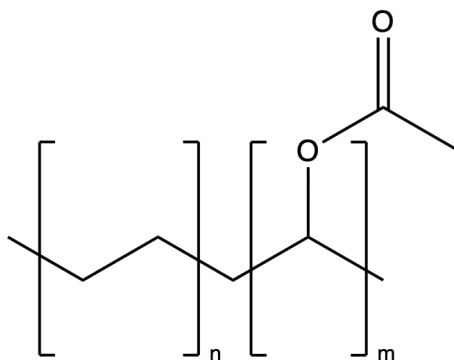


**Figure 5.** Monomeric structure of EVA, consisting of ethylene (left) and vinyl acetate (right).

In order to remove the EVA encapsulant and increase the purity of recovered materials, making recycling more economically viable, chemical separation methods have been widely researched. Because the polymer adhesive is cross-linked, it is challenging to remove without the use of chemical or thermal treatments, as discussed previously. Though many researchers have reported some success in EVA removal for solar panel recycling, they often use harmful chemicals or generate harmful byproducts, which create challenges when considering scaling these methods to the industrial level that would be needed to address the issue of PV waste.

Organic solvents are highly researched in the literature. Submerging a solar panel in solvents such as tetrahydrofuran, trichloroethylene, o-dichlorobenzene, and toluene resulted in a chemical breakdown of EVA, and immersing the panel in toluene at 90 °C for 2 days separated the silicon cell from the glass layer, but did not fully dissolve EVA, which was subsequently thermally removed (Kang et al., 2012). Trichloroethylene, o-dichlorobenzene, benzene, and toluene in combination with ultrasonic radiation at 450 W was effective at dissolving EVA at 70 °C in 60 minutes (Y. Kim & Lee, 2012). Ultrasound at 200 W was also used by Azeumo et al., where EVA was dissolved in toluene at 60 °C in less than 60 minutes; xylene was also able to

dissolve EVA (Azeumo et al., 2019). Though many of these experiments show promising results for methods of EVA dissolution and solar panel recycling, the lifecycle and potential negative impacts of the chemicals used are typically not considered.

Sequential electrowinning can be used to separate and extract multiple valuable/toxic metals from the PV module, such as Ag, Cu, and Pb (Huang et al., 2017). This uses a three-electrode electrolyzer (similar in operation to a cyclic voltammetry system), where the silicon wafer is submerged in a leaching solution, here  $\text{HNO}_3$ , and the voltage is swept by a potentiostat. The metals are deposited one at a time on the working electrode, which has an increasingly negative potential applied to it (Huang et al., 2017). While processes such as this one exist which make solar recycling economically viable, this proposed process produces several harmful byproducts, including HF, which require further treatment and chemical scrubbers in order to prevent release into the environment.

### *Green Solvents and Criteria for Solvent Harm*

Many solvents currently used for solar panel recycling are hazardous to humans and the environment. For example, one of the most commonly used solvents for EVA removal in literature is toluene (Kang et al., 2012). According to the EPA, exposure to toluene in moderate or even low doses has been shown to cause central nervous system dysfunction, narcosis, respiratory infection, and kidney damage, among other toxic effects (US EPA National Center for Environmental Assessment, 2005). Many industrial processes utilize nitric acid or hydrofluoric acid, used to dissolve the EVA so that the solar cells can be extracted and reused, or the silicon wafers can be recovered so new cells can be fabricated (Huang et al., 2017). Hydrofluoric acid in particular can cause severe respiratory damage in short-term exposure, and chronic exposure may

lead to skeletal fluorosis in humans, as well as effects on the lungs, liver, and kidneys in other animals (Hydrogen Fluoride, 2016). Additionally, many processing methods involve the use of high temperatures and high energy use, compounding potential risk factors (Marchetti et al., 2018).

We define “greener solvents” as solvents that have comparatively lower risks to Environment, Health, and Safety (EHS) than those currently in use in industrial practices. When analyzing solvents we considered how they can cause harm and how to compare their potential risks to one another. Our goal was to determine a qualitative comparison between solvents, and we considered their potential harm across the three EHS categories. These categories were referenced from a study on EHS impact during process development, and while we did not directly use their assessment model we considered similar categories such as toxicity, risk to health via exposure, and potential environmental harm when comparing our solvents (Koller et al., 2000).

As for their ability to dissolve, the Hansen Solubility Parameters (HSP) model provides a method for finding solvents similar to EVA. The HSP model is based on an overall solubility parameter  $\delta$  for a molecule, defined as

$$\delta^2 = \delta D^2 + \delta P^2 + \delta H^2 \quad (1)$$

where  $\delta D$ ,  $\delta P$ , and  $\delta H$  represent the contribution of dispersion, polar, and hydrogen bonding forces. The HSP distance between two molecules measures their similarity, with a smaller distance meaning greater compatibility, and is defined as

$$Ra^2 = 4(\delta D_1 - \delta D_2)^2 + (\delta P_1 - \delta P_2)^2 + (\delta H_1 - \delta H_2)^2 \quad (2)$$

where the subscript 1 denotes parameters for one molecule and 2 for the other (Díaz de los Ríos et al., 2020). Molecules can be visualized in an HSP space with three axes of  $\delta D$ ,  $\delta P$ , and  $\delta H$ .

By using the HSP model and considering the EHS qualities of the solvents currently used in industry and those proposed in the literature, we identified several possible candidates for solvents that might successfully remove EVA from the solar panel while minimizing the potential for environmental harm. Though many previous studies have looked into chemical treatments for the dissolution of EVA, in conjunction with thermal treatments for PV recycling, most do not consider the environmental impacts of their proposed chemical treatments or the energy consumption of their thermal treatments. We consider the lifecycle impact of this process, not just at the laboratory scale but at the industrial scale. By ensuring that our solvent choices minimize potential negative environmental impacts and that no harmful chemical byproducts are formed in the process, we propose only treatments that can be used for the recycling of photovoltaics without introducing additional negative environmental impacts as a waste treatment process.

### *Policies and Adoption*

This study addresses the technical feasibility of solar recycling, but its implementation also depends heavily on environmental policy decisions. Across the globe, governments have increasingly adopted policies regulating the disposal of photovoltaic waste. Within the United States, 12 state governments have passed legislation addressing the issue to varying extents. Many have only charged state authorities with reviewing the issue and establishing guidelines, but others have begun requiring decommissioning plans for solar installations (Council of State Governments, 2022; Snead, 2021). In California, with the highest number of solar installations in the nation, there is only one in-state recycling plant; within the state, the only alternative is sending the panels to landfills if they are declared non-hazardous, a process that costs firms about

\$1,500 or more (Hurdle, 2023). The state of Washington introduced an extended producer responsibility (EPR) program in 2017 covering both residential and large-scale installations and making manufacturers responsible for the disposal of their panels (Snead, 2021), the first state to make such a program in the nation. Though not statewide, Niagara Falls County, New York, also adopted an EPR program in 2021 (Hutchinson, 2023). Maine took its own approach by establishing a residential fee for installations to help cover recycling costs (Council of State Governments, 2022).

Both New York State and Minnesota have considered but rejected their own EPR programs. California legislators proposed a bill to establish a program in December 2022, though the legislative session ended before it was considered (Hutchinson, 2023). The outcomes of the recent and future policies are yet to be seen, especially as the European Union—having had photovoltaic waste laws since 2012—continues to share a similar recycling rate of roughly 10% with the United States, despite the latter’s relative lack in policy (Hurdle, 2023).

In the private industry, there are several firms that practice photovoltaic recycling. Texas is home to SolarCycle, a firm that shreds panels and with its patented processes to recover primarily glass, low-grade aluminum, copper, silver, and crystalline silicon claims a high recovery rate of those materials (Hurdle, 2023). Another American firm, First Solar, recycles glass, encapsulant, and semiconductor material while claiming a roughly 90% recycling rate for its products. For their cadmium telluride (CdTe) panels, this entails a three-step process, beginning with the crushing and shredding of the entire panel, chemical processes to separate the glass, and then further chemical processes applied to the semiconductor material for recovery. It also offers contractual recycling (Bomgardner, 2018). In Europe, the French firm ROSI focuses on silicon and silver recovery using thermal and soft chemical processes to maintain low

operating costs. In particular, the firm uses pyrolysis to isolate several metals that comprise the panel (Beyer, 2022).

The use of solvents in recycling introduces further waste concerns, as those chemicals must also be properly discarded. As a hazardous material, there are additional environmental policies that cover its disposal. Thermal destruction is typically used to lower waste volumes, though this process poses its own environmental hazards. Existing legislation in the United States gives the Environmental Protection Agency authority over solvent disposal and recycling policy, and it cooperates with the states on the matter, with each government required to have a solvent recovery program (Aboagye et al., 2021). This adds an environmental factor for the solvent no matter how green it is—though the recycling process of the photovoltaic panel is still the primary focus, any methods using solvents must consider the chemicals' impacts as well.

## Methodology

### *Solvent Selection for Chemical Testing*

To find greener solvents that facilitate EVA removal, we considered both their similarity to EVA through the Hansen Solubility Parameters model and their EHS qualities and life-cycle impact. We located the coordinates of a wide range of common solvents as well as several novel green solvents in the Hansen solubility space and compared these to the position of EVA (Díaz de los Ríos et al., 2020). The similarity between a solvent and EVA was calculated following Equation 2 and is shown in Figure 6, with more similar solvents being more likely to dissolve EVA.

Following these criteria and a literature search for eco-friendly solvents, we chose four novel green solvents, d-limonene, 2-methyltetrahydrofuran (2-MeTHF), ethyl oleate, and Cyrene to test experimentally. Min et al. 2023 found that Ethylene glycol diacetate (EGDA) effectively induced separation of the silicon wafer and glass from the EVA layer in tested solar cells. Based on these findings, EGDA was also tested using our methodology. In addition, we tested two solvents as controls, water and toluene. HSP values for each solvent were calculated based on literature sources: Sherwood et al. 2014, Supplemental Information (Cyrene), Date et al. 2011 (Water), Sicaire et al. 2014, (2-methyltetrahydrofuran), Abbott 2024 (d-Limonene) and Dow Haltermann Custom Processing (Ethylene glycol diacetate). d-limonene has the most similarity to EVA based on its HSP distance, followed by toluene, ethyl oleate, 2-MeTHF, Cyrene, EGDA, and lastly water. The structures of these solvents are shown in Figure 7.

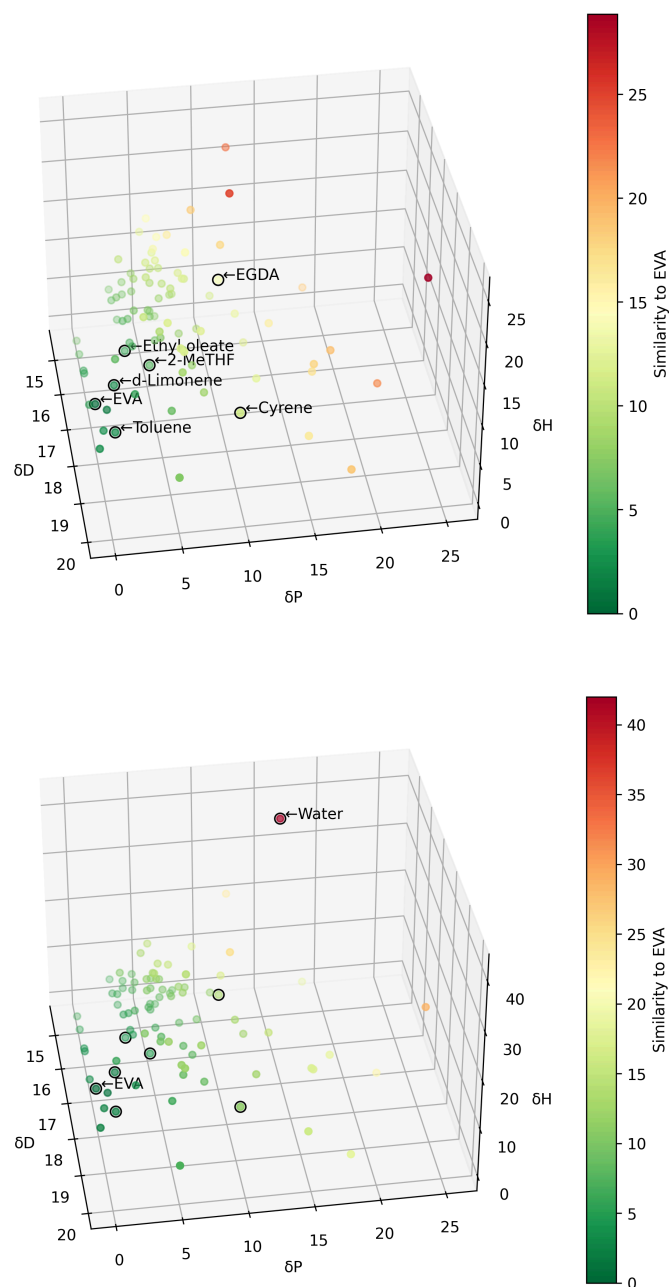


**Figure 6.** 3D plot of Hansen solubility parameters for a range of solvents, colored by their similarity to EVA, with a smaller similarity value being more similar. Seven solvents of note are circled and labeled. Top: Solvents excluding water, for clarity. Bottom: Solvents including water.

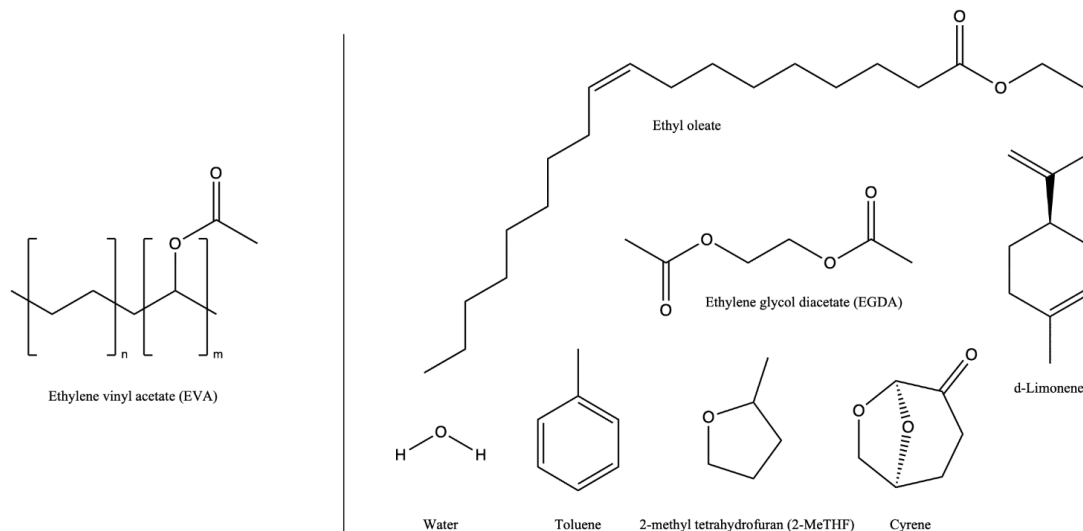


**Figure 7.** Chemical structures of EVA (left) and seven examined solvents (right).

### Water

Water was chosen as a negative control due to its low compatibility with EVA (Figure 6).

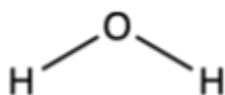


**Figure 8.** Chemical structure of water.

### Toluene

Toluene was chosen as our main control solvent due to its proven effectiveness in removing EVA from solar panels (Kang et al., 2012; Y. Kim & Lee, 2012; Azeumo et al., 2019). It is commonly used as a solvent in the coatings, adhesives, pharmaceuticals, and other industries and has a high worldwide production of 31.26 million tonnes/year, making its introduction in the solar recycling industry easily feasible. However, toluene is highly toxic, readily absorbed by inhalation or skin

absorption to cause systemic toxicity with negative effects on the central nervous system, cardiovascular system, reproductive system, and digestive system (Medical Management Guidelines for Toluene, 2014). It has a short half-life in the environment (5 hours in water, 14 hours in the atmosphere) but does have moderate acute and chronic toxicity for aquatic life. It is also derived mainly from the refining of crude petroleum by catalytic reforming or hydrocracking of heavier hydrocarbons. Toluene is disposed of by controlled incineration. For these reasons, we searched for solvents that might have similar effects on EVA as toluene that are safer for humans and the environment.

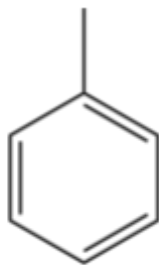


**Figure 9.** Chemical structure of toluene.

### **d-Limonene**

d-Limonene was shown to have the most similarity to EVA in the Hansen Solubility Parameters model. Derived from the oil from citrus fruit peels by steam distillation, it is a common green solvent used for cleaning, flavoring, and chemical processing applications (Sharma et al., 2017). It is used extensively as a flavor and fragrance additive, a solvent and cleaner, and insect repellent with a worldwide production of 50,000 tonnes/year. High concentrations of the chemical produce harmful biological effects and it is considered highly toxic for aquatic life, but no human toxicity similar to toluene has been reported and the lower dose threshold for effects is lower than that of

toluene (d-Limonene, 1993). Notably, the chemical is allowed as a food additive by the FDA (d-Limonene, 1993). The main danger of contact is skin irritation.

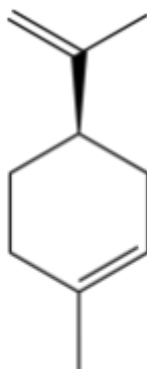


**Figure 10.** Chemical structure of d-limonene.

### **2-methyltetrahydrofuran (2-MeTHF)**

Tetrahydrofuran has previously been tested for the removal of EVA from solar panels. It is relatively nontoxic compared to solvents like toluene, causing skin irritation and eye damage on contact but having low acute toxicity (Fowles, 2013). However, the main production method for tetrahydrofuran is the dehydration of 1,4-butanediol, which is synthesized from fossil fuels (Tetrahydrofuran, 2015). 2-methyltetrahydrofuran differs from tetrahydrofuran by one methyl group and is renewable, produced from the hydrogenation of furfural, which is derived from the dehydration of xylose from hemicellulose in biomass (Sicaire, 2014). It has been examined as a greener and safer replacement for similar organic solvents in organic synthesis applications, however, it is still a relatively novel solvent and its production may have to be increased before its use is feasible.



**Figure 11.** Chemical structure of 2-MeTHF.

## Cyrene

Cyrene, or dihydrolevoglucosenone, is a bio-based solvent developed as an alternative to dipolar aprotic solvents, which are similar to moderately polar aprotic solvents like tetrahydrofuran. It is renewable and produced by hydrogenating levoglucosenone, which is from the acid-catalyzed pyrolysis of cellulose (Sherwood et. al., 2014). It is a novel solvent marketed as a substitute for petrochemical-derived solvents and its large-scale production is still under development.

Environmental and human health effects other than eye irritation have not been fully investigated.

Methods of disposal include incineration.

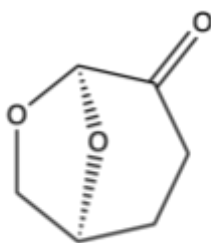


**Figure 12.** Chemical structure of cyrene.

## Ethyl oleate

Ethyl oleate, a fatty acid ester used as a food additive, solvent, and drug delivery agent, is an extremely safe solvent that is still fairly similar to EVA by the Hansen solubility parameters model (Bookstaff, 2003). It is produced by the esterification of oleic acid, which is the most

common fatty acid in nature and can be purified from vegetable oils. It has no reported environmental or human health effects.

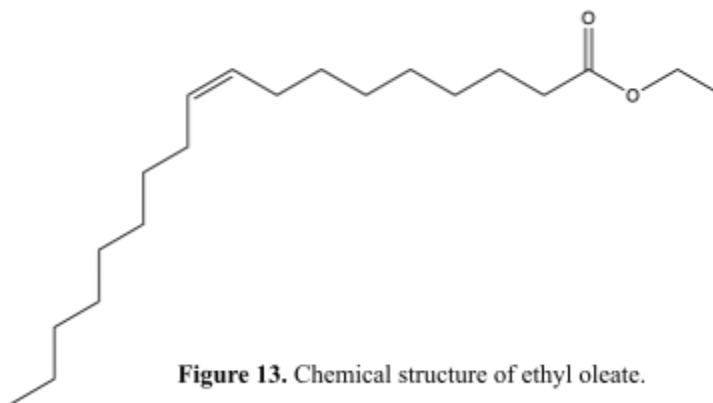


**Figure 13.** Chemical structure of ethyl oleate.

### **Ethylene glycol diacetate (EGDA)**

Ethylene glycol diacetate is one solvent that has been previously investigated as a greener solvent for photovoltaic recycling (Min et al., 2023). Notably, while most studies on photovoltaic recycling focus on dissolving EVA, Min et al. found that treating panels with EGDA allows the EVA layers to be peeled apart without significant mechanical deformation. It is produced by the esterification of ethylene glycol, which is synthesized from ethylene, a product of petroleum refining. It is often used as a solvent and plasticizer and has no reported environmental or human health effects other than eye irritation, and is believed to be biodegradable. While its Hansen solubility parameters are not as close to EVA, it does have a similar chemical structure as both contain ethyl acetate.

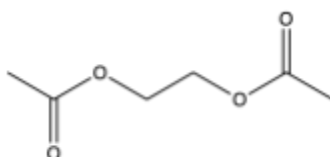


**Figure 14.** Chemical structure of EGDA.

70°C was chosen as the initial testing temperature to maintain consistency with treatment conditions in published solvent efficacy experiments (Kang et al. 2012). In order to study the effect of temperature on encapsulant removal, temperatures in the 70°C-190°C range were tested. Within this range, each solvent was only tested at temperatures below its boiling point, as shown in Table 1 below.

**Table 1.** Table of solvent boiling points and temperatures at which they were tested.

<b>Solvent</b>	<b>Boiling point</b>	<b>Testing temperatures</b>
Water	100°C (Water, 2024)	70 °C
Toluene	110.6°C (Toluene, 2024)	70 °C, 100 °C
d-Limonene	177.6°C (Limonene, (+)-, 2024)	70 °C, 100 °C, 130 °C, 160 °C
Ethyl oleate	206.55°C (Ethyl Oleate, 2023)	70 °C
2-MeTHF	80.2 °C (Aycok, 2007)	70 °C
EGDA	190-191°C (Ethylene glycol diacetate, 2024)	70 °C, 100 °C, 130 °C
Cyrene	227 °C (Citarella, 2022)	70 °C, 130 °C, 160 °C, 190 °C

### *Panel Disassembly and Sample Preparation*

Two types of samples were prepared for solvent testing: EVA film and solar panel fragments. Pieces of EVA film measuring approximately 2 x 2 cm were cut and weighed. For the panel fragments, the aluminum frame and junction box were removed from monocrystalline solar panels purchased from NewPowa prior to cutting.

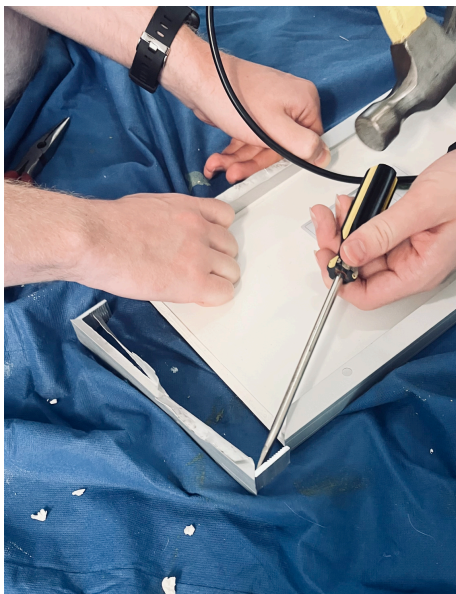


**Figure 15.** Mechanical removal of the aluminum frame from the solar panel.

Solar panel fragments were extracted by breaking and removing the top glass layer by mechanical force, then cutting the more flexible remnants into smaller pieces using scissors. All solvent tests were conducted on fragments extracted in this manner. Since the goal of the study was to focus on interactions between each solvent and the EVA encapsulant, all tested fragments had no top glass layer and consisted only of the backsheet, internal circuitry, silicon wafer, and the connecting EVA layers above and below the silicon wafer.

These fragments do not perfectly model the effect that various solvents would have on a full solar panel. The glass top layer is removed from these samples. If present, this layer would significantly reduce the solvent-EVA contact area. Additionally, the mechanical breakdown process, especially the process of cutting the cell into fragments, compromises the integrity of the brittle silicon wafers, preventing the recovery of unbroken silicon wafers.

For a more accurate extraction that retains the glass and keeps the wafers intact, we investigated coring the panels. The cores would accurately represent a small-scale model of a full

solar panel with the aluminum frame and junction box removed, consisting of glass, EVA, silicon cells, internal circuitry, and the back sheet, and would allow for more representative solvent testing at the laboratory scale. There are several ways to core a solar panel, including full coring, which cuts all the way through the panel, and partial coring, which leaves the glass layer intact (Moutinho et al., 2020). Since glass-on samples were desired, full coring was chosen. To core the solar panel, the aluminum frame and junction box were removed. The coring capabilities of a JET Drill mill and an OMAX ProtoMAX water jet were tested. The drill mill was used with a diamond-tipped hole saw. This process required more effort from the user and often broke the glass. The water jet consistently cracked the glass but enabled the recovery of a functional core (Figure 16). The water jet also operated at higher speeds than the drill mill. Ultimately, the water jet was established as the better choice for this application. Although these cores were not used in our experiments, it is important to note as a nondestructive sampling technique.

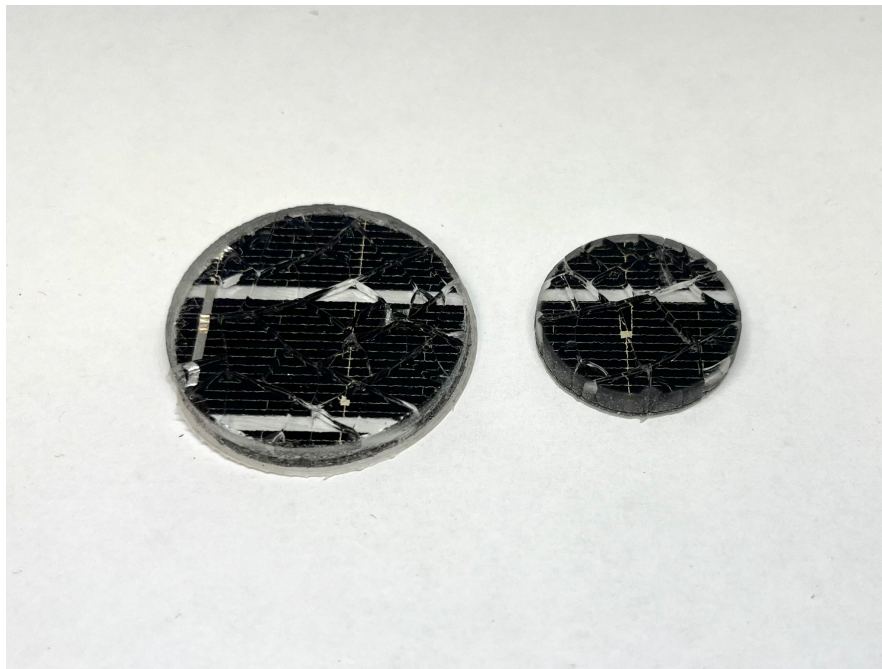


**Figure 16.** Solar panel cores of diameter 4 cm and 2 cm.

### *Solvent Testing Procedure*

We investigated the effect of solvents on both EVA film pieces and solar panel fragments. EVA film pieces were cut from a roll. After measuring the initial weight, each sample piece was placed in a beaker with solvent at temperatures listed in Table 1 for 5 hours with a magnetic stir bar. Samples were tested at a range of temperatures described in Table 1, with the upper limit determined by the solvent's boiling point. Hot plate temperature was controlled with a thermocouple. Two samples were placed on the hot plate for each test. The solvent volume was held constant with respect to sample mass, with 0.0015 g sample/mL solvent for the EVA film tests and 0.003 g sample/mL solvent for the solar panel fragment tests. All solvent types employed the same ratio. Following solvent treatment, the contents of each beaker were vacuum-filtered to collect all remaining solids. Samples were then left to dry ambiently and in a vacuum oven at 24 inHg and 75°C before the final weight was taken. Percent change in mass was calculated using the following equation:

$$\frac{\text{original mass} - \text{final mass}}{\text{original mass}} * 100$$

Toluene was sourced from Fisher Scientific; 2-MeTHF, Cyrene, and EGDA from Sigma Aldrich; d-limonene from JSP; and 70% technical grade ethyl oleate from Beantown Chemical.

### *Gasification Procedure*

The ethylene vinyl acetate (EVA) used for gasification was shredded into pieces approximately 2 x 2 mm and used for thermogravimetric analysis (TGA) and to examine gasification behavior. Thermogravimetric analysis is a means of measuring the mass of a sample over a temperature range. This is a means to characterize the sample's thermal behavior. Such experiments were conducted using an SDT Q600 (manufactured by Texas Instruments) which is

capable of differential scanning calorimetry (DSC) and TGA. In the three TGA tests, samples of EVA film were crushed into a fine powder, and sample masses of 4.7510, 4.4810, and 4.0440 mg were used for trials 1, 2, and 3 respectively. Argon was used as the purge gas and flowed at a rate of 100 mL/min. Starting from room temperature (20° C), the sample was heated to 105°C and held at that temperature isothermally for 10 minutes. Afterward, the sample was heated at a rate of 20°C/min until 950°C was reached. Again, equilibrating at 950°C occurs and it was isothermally held here for 10 minutes. Air was then used instead of argon as the purge gas and the system was isothermal for the final 10 minutes. The experiment lasted for 80 minutes and was repeated for three trials. The sample holder pans were kept open without caps to prevent interference during the devolatilization process. The procedure outlined here follows a similar process as ASTM 7582-15, the Standard for Test Methods for Proximate Analysis of Coal and Coke by Macro Thermogravimetric Analysis (ASTM International 2023).

Gasification experiments were conducted in a laboratory semi-batch reactor facility.

Figure 17 below is a schematic outline of the facility. For gasification, a 10 g EVA sample (again, shredded into a fine powder) was used. Nitrogen and CO<sub>2</sub> were used as the gasifying agents.

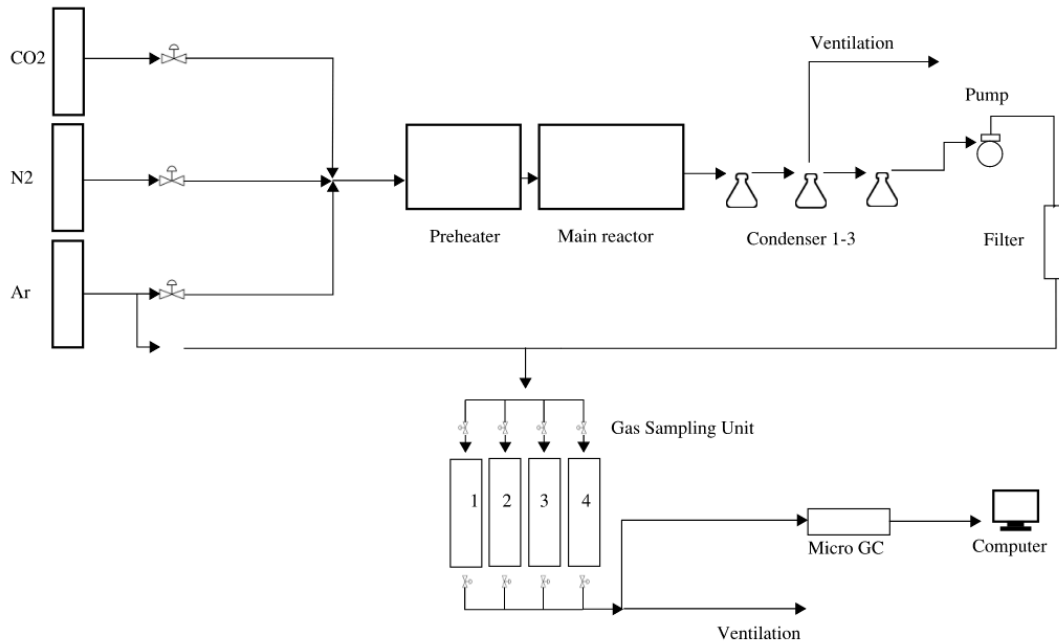


**Figure 17.** Schematic of gasification experiment.

Gasification experiments were completed following the previous gasification experimental procedures and laboratory space offered by Dr. Ashwani K. Gupta, a University of Maryland Mechanical Engineering professor (Mavukwana et al., 2023). As shown in Figure 17, a horizontal furnace pre-heated the gasifying agents and feedstock. The preheater furnace (Lindberg) prior to the main reactor ensured that the carrier gases were heated to the desired temperature. With the preheater and main reactor set at the same temperature, the EVA sample was placed inside the main reactor via a coupling (Policella et al., 2019). The sample was loaded in a stainless-steel circular mesh. At this point, the system split into a bypass line and a sampling line. The majority of the gas mixture entered the bypass line and exited through the exhaust. In the sampling line, evolved gases from the gasification passed through an ice bath condenser. A filter then removed any water droplets and tar. After passing through the three condensers, a micro gas chromatograph (micro GC) was used to analyze product gas composition. At 0.5, 1, 2,

3, and 4 minutes, samples were collected within each of the five gas sampling cylinders respectively. The GC analysis began at approximately 5 minutes. Using knowledge of the flow rate of the tracer gas (N<sub>2</sub>), the flow rates of the resulting gases from the GC were determined.

Following an ideal gas assumption, the mass flow rates for each detected gas were calculated as

$$M_i = \frac{X_i}{X_{N_2}} V_{N_2} \rho_i \quad (1)$$

where  $M_i$  is the mass flow rate in grams per second,  $X_i$  is the mole fraction of a given species,  $X_{N_2}$  is the mole fraction of N<sub>2</sub>, and  $\rho_i$  is the species density at standard temperature and pressure.

Within the Agilent 3000A microGC, the thermal conductivity detector made for calibrating the gasses ensured repeatability (Policella et al., 2019).

As for experimental conditions, 2.1 standard liters per minute (slpm) of 75% vol CO<sub>2</sub> and 25% vol N<sub>2</sub> mixture (at standard 293 K and 1 atm) was used for tracer gas and inert medium as indicated in Table 2. Before the experiment, the system was flushed with argon gas to ensure a clean system free from any residues from past runs (Policella et al., 2019).

**Table 2.** Gasification experimental parameters.

Reactor Temperature	900°C
Operating Pressure	Atmospheric
Tracer Gas and Inert Medium	2.1 slpm of 75% vol CO <sub>2</sub> and 25% vol N <sub>2</sub> mixture (at standard 293 K and 1 atm)
Sample	10 g of EVA 2 x 2 mm pieces
Isothermal Reaction Time	45 min

## Results & Discussion

### *Solvent Testing*

Figures 18 and 19 below show the summary of results for both the EVA film and solar panel fragment experiments for each solvent. Percent weight loss calculations were carried out by massing the solar panel before and after chemical treatment, as an indication of how much EVA was dissolved in the solution, discussed further later.

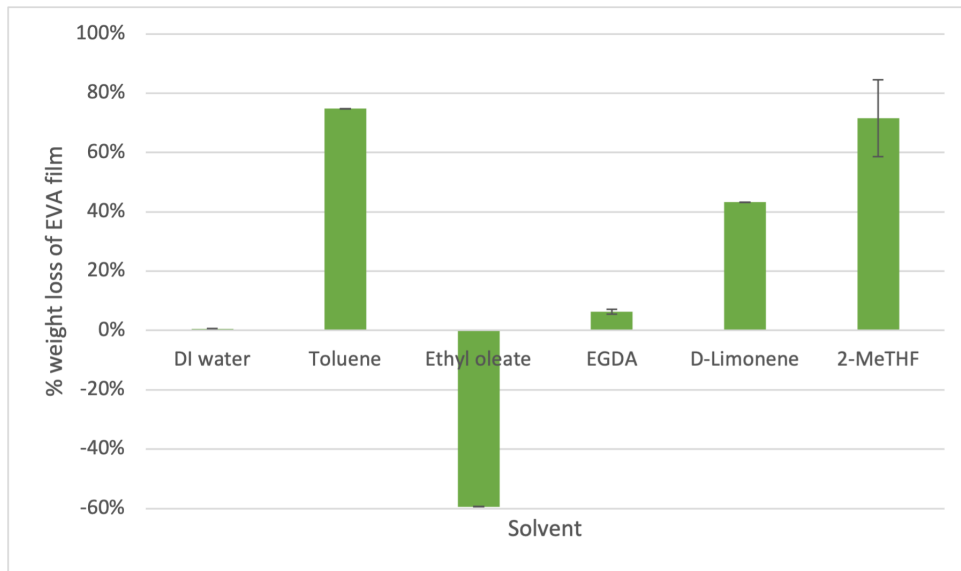


**Figure 18.** Results of solvent testing showing % weight loss by solvent for EVA film samples.

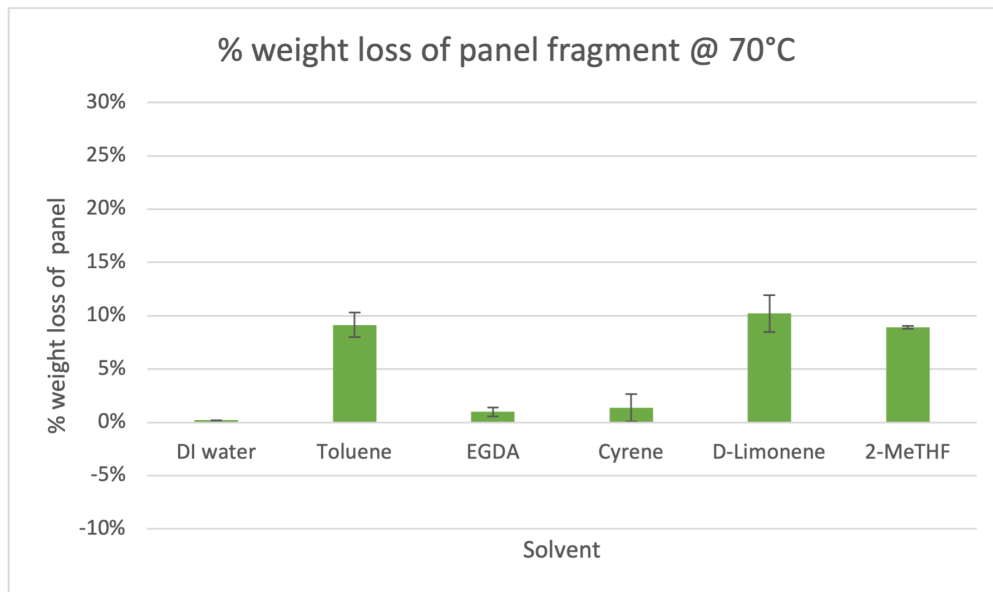


**Figure 19.** Results of solvent testing showing % weight loss by solvent for solar panel samples.

For those solvents that showed promising results, we completed chemical dissolution experiments in conjunction with thermal experiments, i.e. we tested their dissolution capabilities at different temperatures, as shown in Figure 20 below.

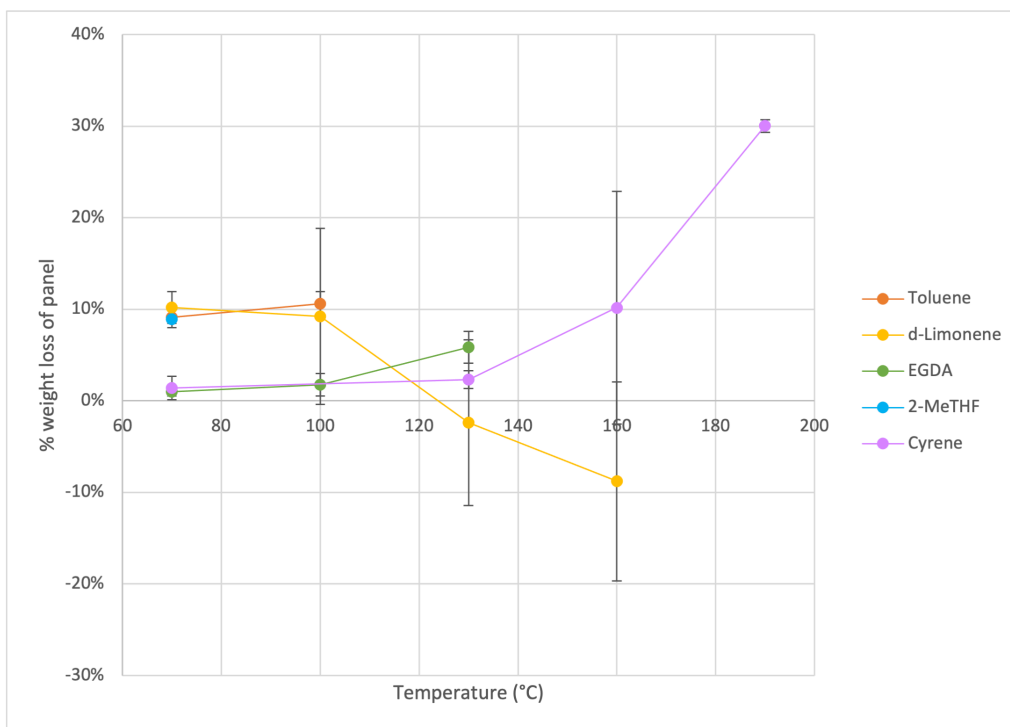


**Figure 20.** Results of solvent testing for solar panel samples at different temperatures.

In addition to mass loss results, we include images of the solar panel before (Figure 21) and after chemical treatment for each solvent and at different temperatures. These images are useful to qualitatively demonstrate how well the solvent dissolved EVA.

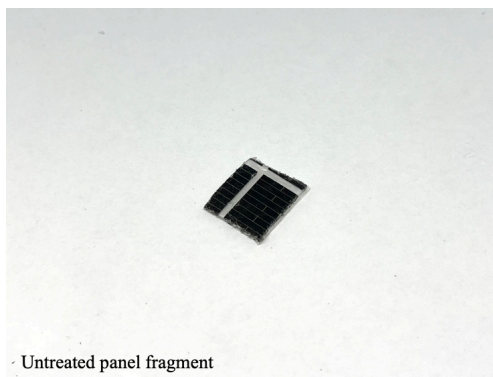


**Figure 21.** Image of a solar panel fragment after sample preparation as described above.

For each solvent we include a plot of the percent mass loss as a function of temperature, as well as the “after” images, following solvent testing. As mentioned previously, toluene has been extensively used in the literature and was used as our standard. Water was used as a control. A panel fragment treated with 70°C water for 5 hours had no noticeable changes in appearance and showed a % mass loss of just 0.19%. This indicates that heat alone is not enough to facilitate panel breakdown, and a compatible solvent must be present.

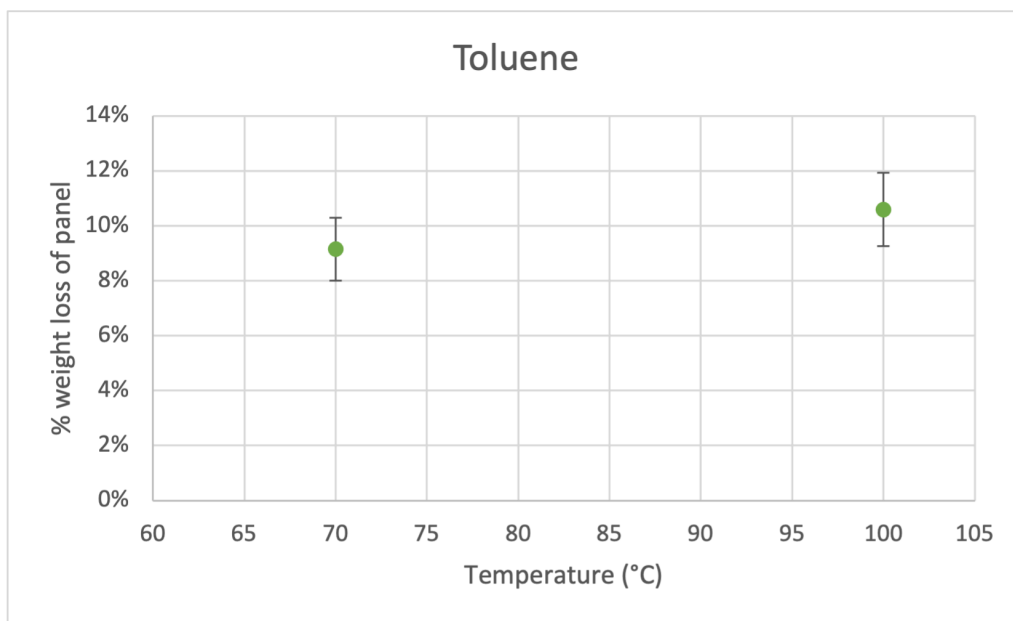


**Figure 22.** % weight loss results for solar panel submerged in toluene at different temperatures.

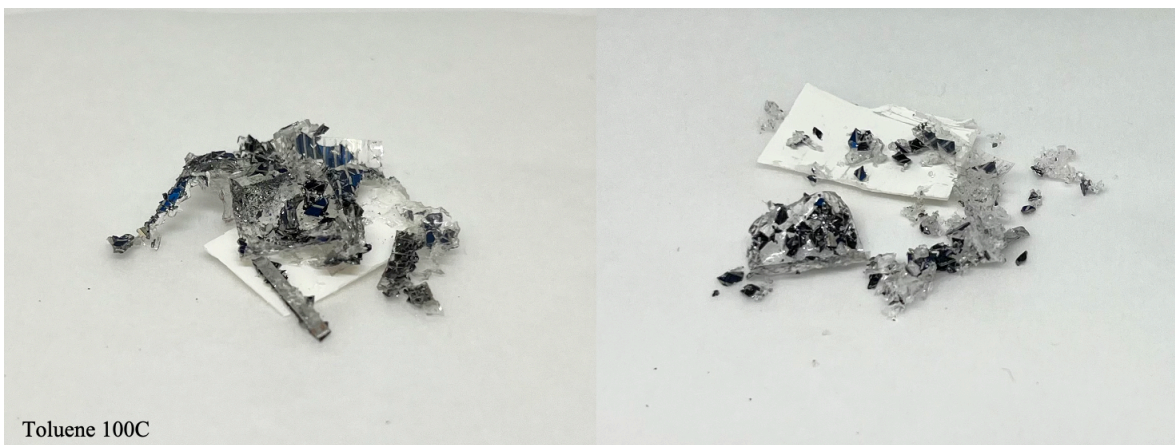


**Figure 23.** Solar panel fragments following toluene treatment at 100°C.

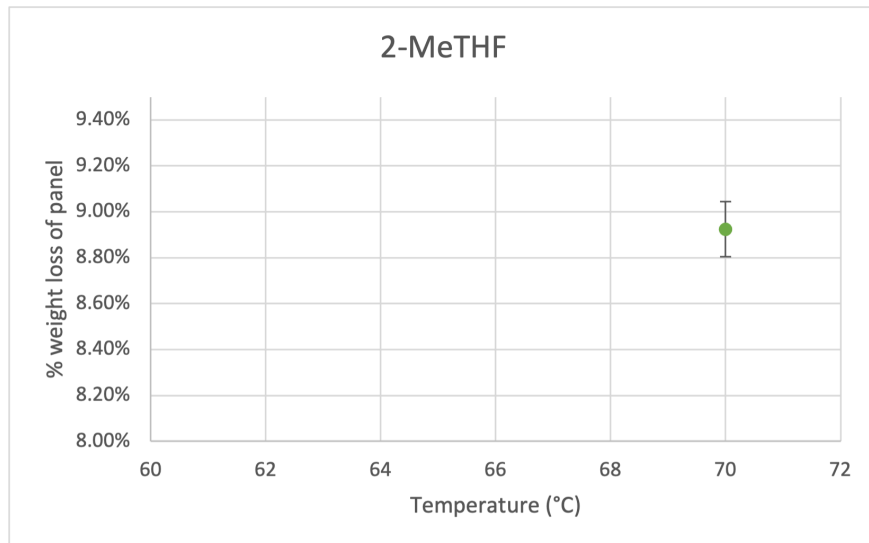


**Figure 24.** % weight loss results for solar panel submerged in 2-MeTHF.



**Figure 25.** Solar panel fragments following 2-MeTHF treatment at 70°C.

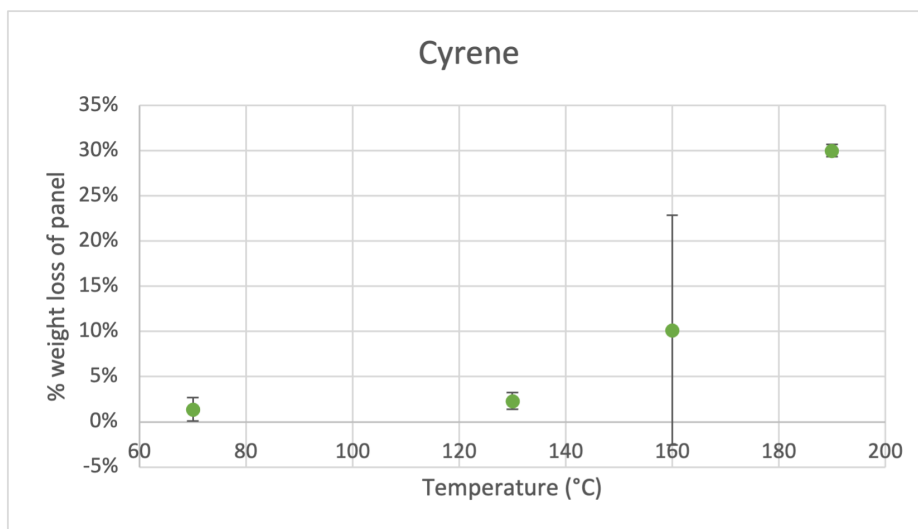


**Figure 26.** % weight loss results for solar panel submerged in Cyrene at various temperatures.

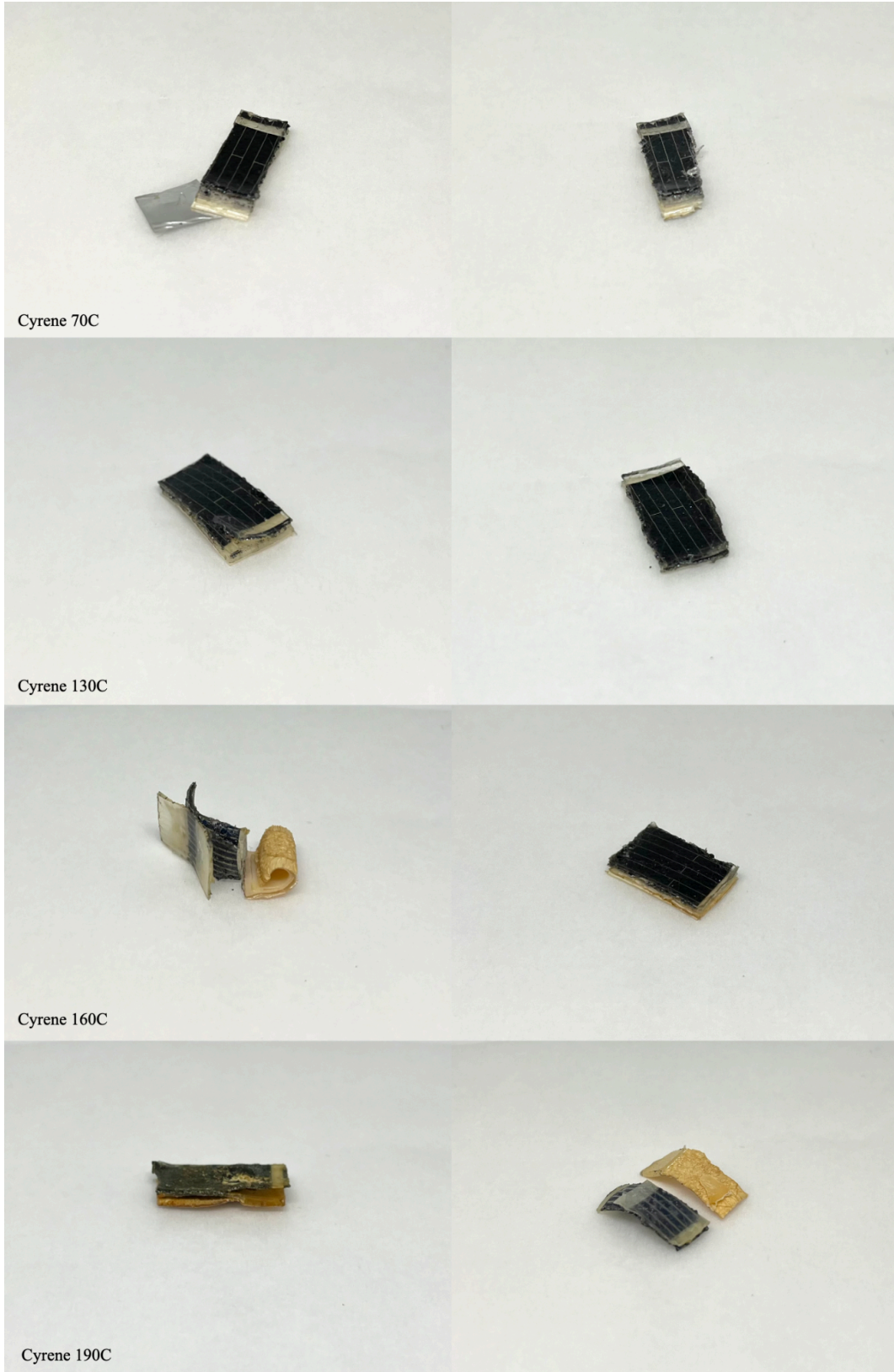


**Figure 27.** Solar panel fragments following Cyrene treatment at various temperatures.

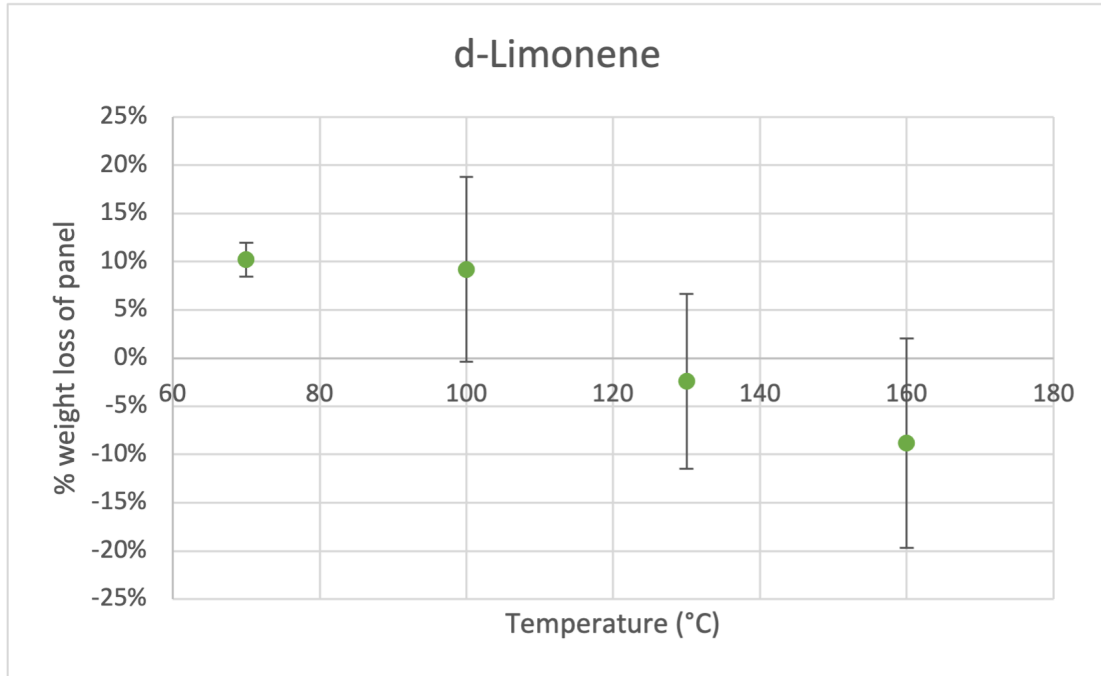


**Figure 28.** % weight loss results for solar panel submerged in d-limonene at various temperatures.

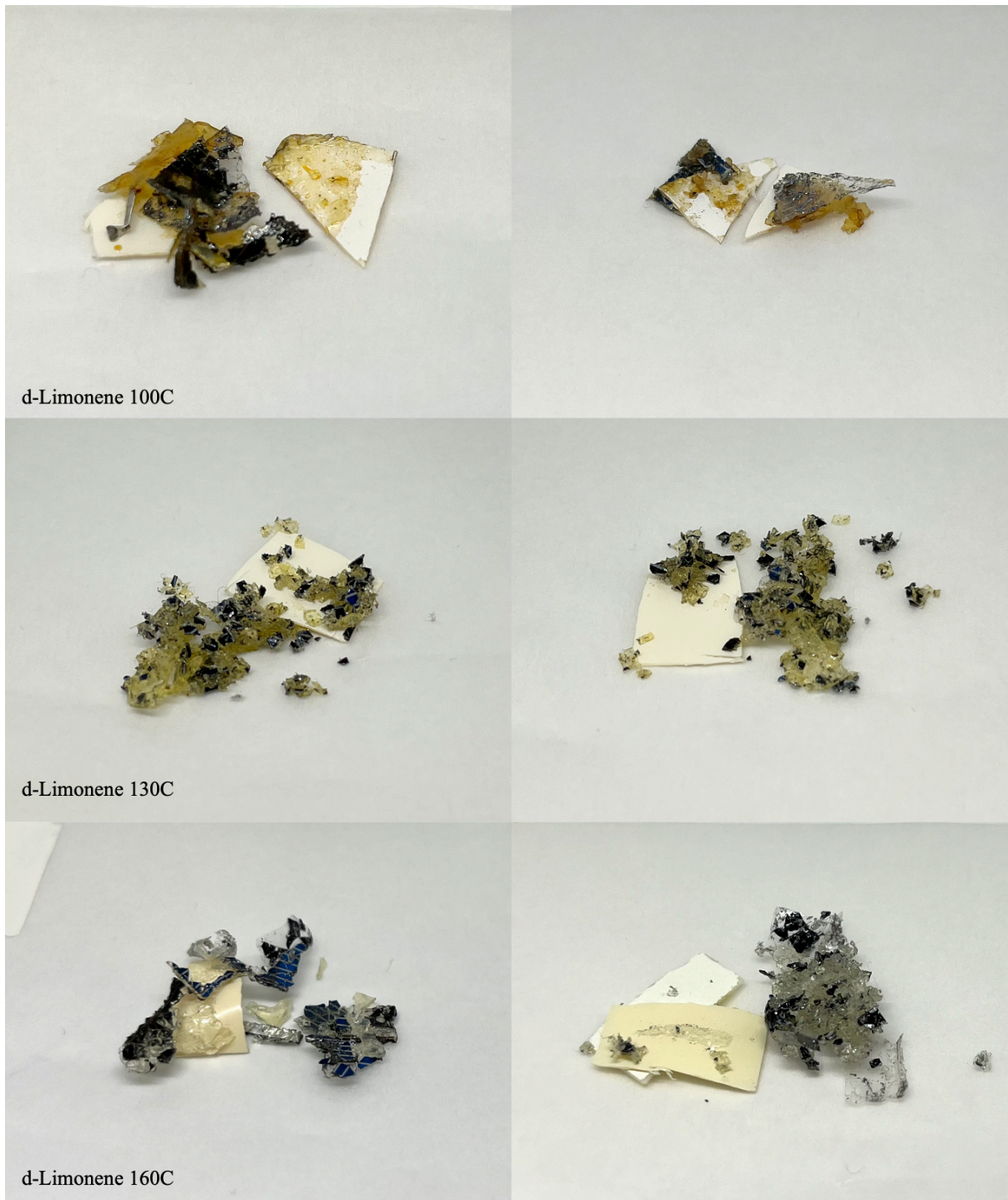


**Figure 29.** Solar panel fragments following d-limonene treatment at various temperatures.

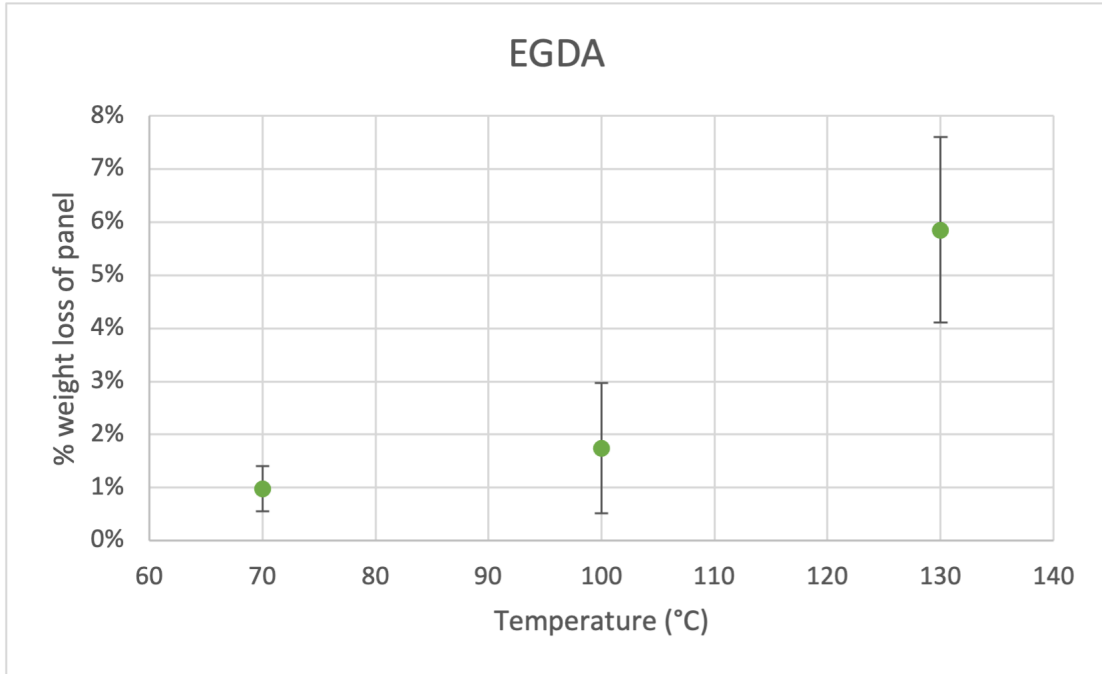


**Figure 30** % weight loss results for solar panel submerged in EGDA at various temperatures.

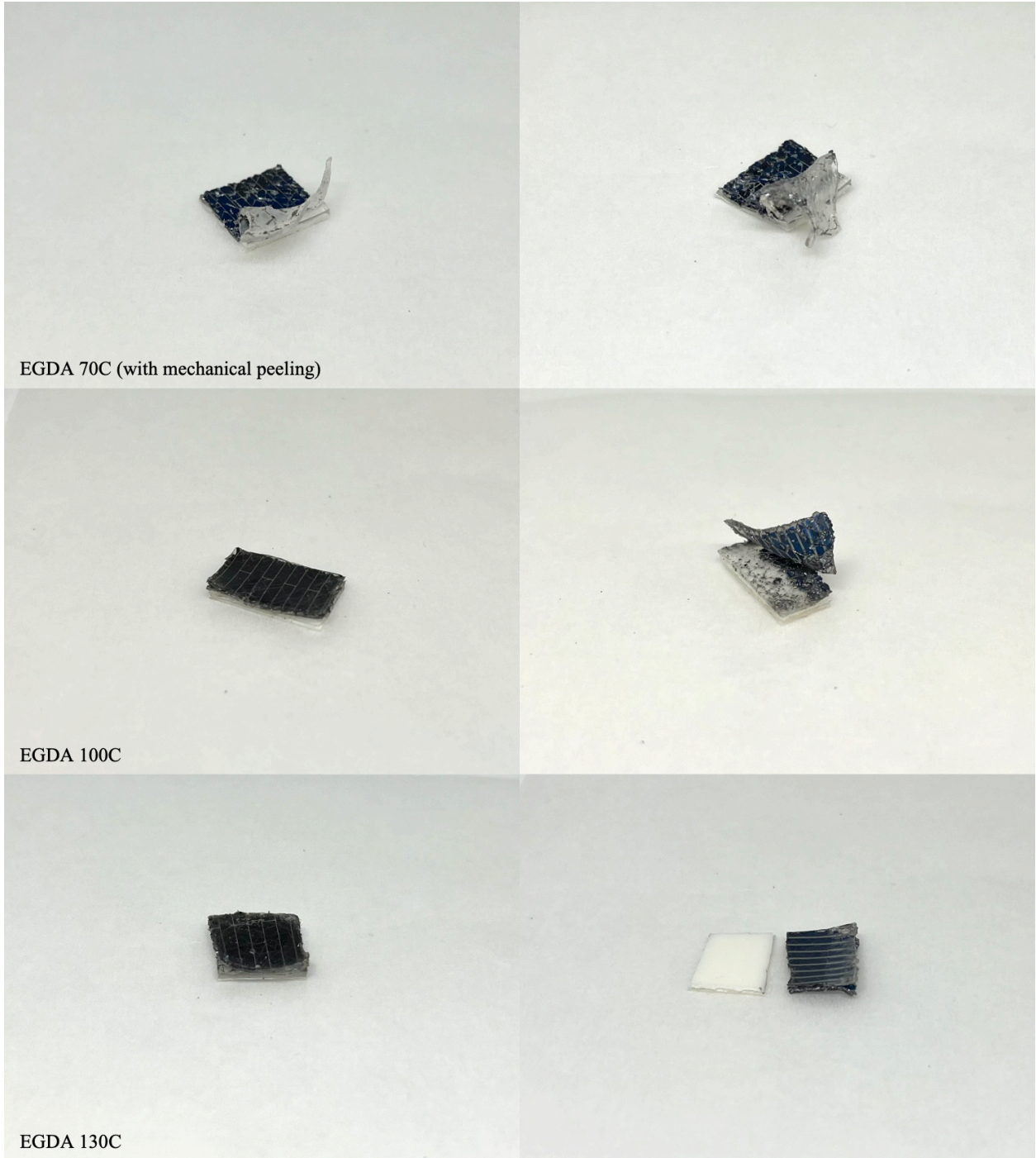


**Figure 31.** Solar panel fragments following EDGA treatment at various temperatures.

The mass loss data above is presented in conjunction with post-treatment images, as mass loss alone is an inexact treatment efficacy metric. Even when substantial mechanical breakdown of the EVA was observed, yielding end results visually similar to those of toluene, samples did not have post-treatment mass losses of the same magnitude as those treated in toluene (Figure 20). It's possible that due to crosslinked EVA's tendency to swell rather than dissolve in the presence of solvent, some of the solvents tested are inducing a conformational change but no substantial dissolution, which would cause pre- and post-treatment masses to be equal (Doi et al. 2001, Mencer and Gomzi 1994).

However, several samples increased in mass after treatment, corresponding to a negative percent mass loss. d-Limonene, Cyrene, EGDA samples treated at temperatures greater than or equal to 100°C exhibited an increase in mass after solvent treatment and over a week of drying in ambient air. Once these samples were dried in a vacuum oven environment for 18-20 hours, their masses decreased. This suggests that some solvents remain in the EVA matrix after treatment if the panel is dried at room temperature rather than heat-treated. This is likely caused by a combination of low solvent volatility and high solvent affinity for the polymer matrix—solvents with lower boiling points (i.e. toluene and 2-MeTHF) showed little to no mass increase after treatment, while solvents with high boiling points (d-limonene, Cyrene, EGDA) showed mass increases after treatment and ambient-atmosphere drying, and mass decreases after vacuum oven drying.

It is unclear whether the final recorded mass losses of these samples represent the solvent-free mass, or simply the limit as to what can be removed after drying under the 75°C, 25 inHg vacuum oven conditions. In the case of d-limonene, some solvent clearly remains in the polymer matrix after 18-20 hours of vacuum drying, since samples treated at or above 130°C

show masses higher than their pretreatment mass. D-Limonene has both a high boiling point and a high affinity for EVA as measured by the Hansen Solubility Parameters, making it particularly difficult to remove via evaporation. Higher temperatures and lower pressures may promote a greater degree of EVA/d-limonene interaction, exacerbating this issue and leading to the counterintuitive phenomenon of panel mass loss decreasing with increasing temperature. Thus, although d-limonene showed less mass loss than other solvents at high temperatures, it still shows promise as a toluene alternative due to the degree of conformational change it induced in the panel fragments, shown clearly in Figure 29. Notably, the results from d-limonene at 70°C were similar to those of toluene.

In future studies on this topic, measuring the concentration of dissolved polymer in the post-treatment solvent via FTIR or UV-Vis could help clarify mass-loss results. However, due to the cross-linked nature of EVA, EVA removal is generally facilitated by a combination of chemical dissolution and solvent-aided mechanical breakdown. Thus, chemical measurements should be considered in conjunction with physical measurements if conducted. Chemical analysis techniques are discussed in more detail in the Future Work section. When considering the concentration of dissolved EVA as an alternative metric of experimental success, it's also important to note that some solvents can effectively separate the silicon wafer from the backsheet without fully dissolving the EVA layer or facilitating a large change in panel mass (Figures 30 and 31). Thus, the qualitative photographs are included to provide a more complete understanding of the effects of each solvent.

Notably, high standard deviations (up to 100% of the mean) were observed for select d-limonene, Cyrene, and EGDA samples (Figure 20). In most experiments, two samples were

heated simultaneously in separate beakers on the same hot plate during each 5-hour testing period. The hot plate's temperature probe was placed in the centered beaker. It was predicted that the temperature difference between the two beakers would not be significant enough to affect experimental results. However, as shown in Appendix I, all mass loss results for samples tested in the off-center beaker, which did not contain a temperature probe, were consistent with lower-than-expected treatment temperatures. This suggests that the large variability observed in many of the mass loss results may have been caused by unintended differences in treatment temperatures. The failure of several chemicals to fully evaporate may also have contributed to variation in mass loss. Due to the inconsistent treatment conditions and limited number of replicates, it was difficult to conduct reliable statistical analyses on these datasets. As a result, the significance of the effect of solvent type and temperature was not quantified in this study, and remains an important target for future work. However, general trends can still be observed from mass loss data and post-treatment images.

Considering both mass loss measurements and panel appearance post-treatment, 2-MeTHF produced results most similar to toluene's (Figure 24). However, limitations with mass loss analysis were discussed above. Differences in mass loss may arise in part due to a difference in solvent volatilities and affinities as well as differences in the solvent's effect on EVA. Visually, different solvents showed different panel breakdown mechanisms. Toluene, d-limonene, and 2-MeTHF treatments caused significant, observable conformational changes to the panel (Figures 23, 24, and 29). These solvents reduced adhesion between EVA and silicon as well as silicon and the panel. Silicon fragments with no visible EVA residue were recovered from these samples post-treatment. In contrast, while EGDA and Cyrene treatments generally caused the backsheet to separate from the panel, they did not induce the same degree of conformational change in the

EVA (Figures 27 and 31). The silicon wafers remained embedded in the front EVA layer, now detached from the backsheet. Compared to toluene and d-limonene, EVA was predicted to be less soluble in Cyrene and EGDA, suggesting that this difference in affinity can lead to different panel breakdown mechanisms and a reduction in EVA swelling.

The temperature range at which each solvent could be tested was limited by its boiling point. With the exception of toluene, discussed above, mass loss increased with increasing temperature in all solvents. Cyrene in particular exhibited a large increase (Figure 26 and Appendix 1) in mass loss between 130°C and 190°C, suggesting that the higher temperature introduces new panel/solvent interactions that are particularly favorable for panel breakdown. No clear visual differences were observed between post-treatment panels at different temperatures in toluene, d-limonene, or 2-MeTHF. In Cyrene and EGDA, observation of the treated panel pieces indicated that EVA peeling and backsheet separation became more prevalent at high temperatures. Increasing temperatures promote solvent mobility in the polymer matrix and increase solvent/polymer interactions.

There are advantages to both panel breakdown mechanisms observed in this study. Silicon wafers can be recycled as fragments or in an intact form (Park and Park et al. 2014, Park et al. 2016, Latunussa et al., 2016). The mechanical breakdown processes used in this study apply significant stress to the silicon wafers, causing them to fragment easily when the structural support of the EVA layer is removed. This precludes the possibility of intact wafer recovery. Treating full PV cells with solvent instead of using fragments eliminates the stress that mechanical breakdown places on brittle silicon wafers (Kang et al. 2012). However, previous studies have shown that the swelling behavior of EVA can even cause silicon wafers in full cells

to crack during treatment (Doi et al. 2001). Some researchers have successfully prevented this cracking by applying pressure to the cell throughout the solvent treatment process (Doi et al. 2001).

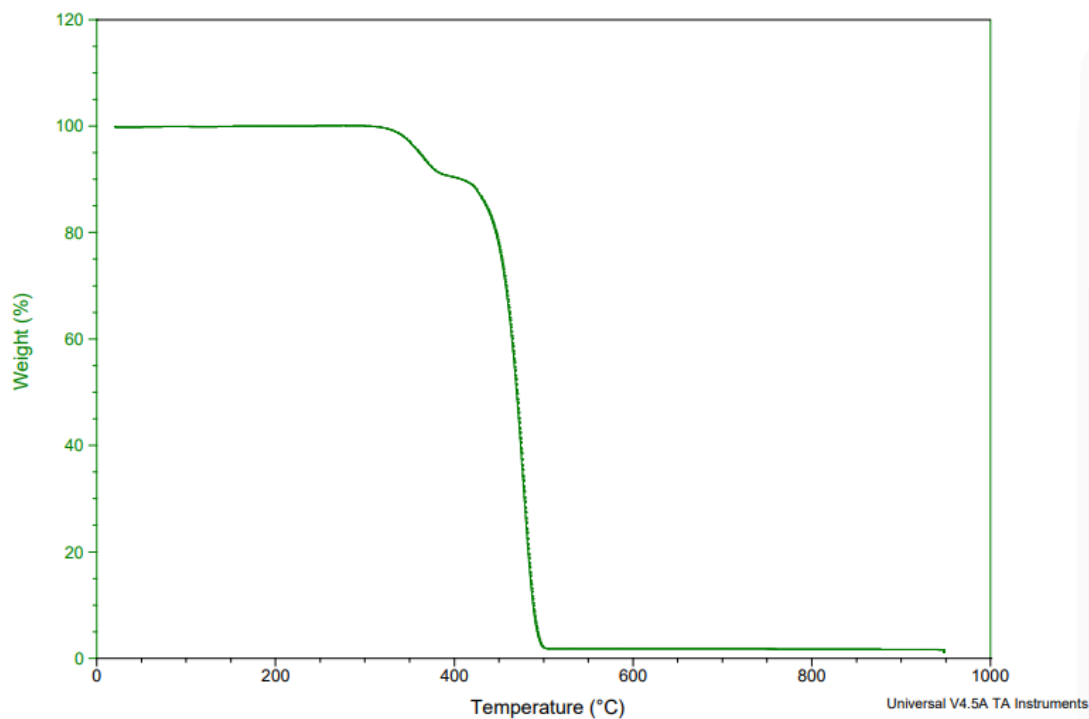
Of the solvents tested, d-limonene and 2-MeTHF are most likely to enable a 1-step disassembly process, separating the backsheets, EVA, and silicon wafer in a single treatment. In contrast, free silicon wafer fragments were not recovered from samples treated with Cyrene and EGDA, suggesting that full separation in one step would be difficult to accomplish regardless of treatment conditions. This does not necessarily preclude these solvents from use in PV recycling. In fact, selectively separating the backsheets could then allow EVA to be removed thermally without generating the harmful fluorinated gas compounds which arise when the backsheets are treated at high temperatures (Dobra et al. 2020). Additionally, Cyrene and EDGA consistently caused less swelling and mechanical deformation than d-limonene and 2-MeTHF, opening a path to intact wafer recovery in full-cell treatments (Min et al. 2023). Notably, none of the solvents, toluene control included, fully removed EVA from the silicon wafer in the 5-hour tests. This outcome was expected, given the difficulty of fully dissolving crosslinked EVA. In previous solvent-based EVA removal studies, EVA remained attached to the silicon wafers even after 2 days of immersion in toluene and was only fully removed by heating the EVA to 600°C for 60 minutes (Kang et al. 2012). In order to facilitate complete EVA removal after solvent treatments have separated the glass and backsheets from the Si wafer, a heating step may need to be added to this process as well.

These results show that several low-hazard and/or renewable solvents show promise as toluene alternatives for solar recycling. However, there are other practical limitations to the use of these solvents in place of toluene. For one, several of them are very expensive. For example,

2-MeTHF costs \$288 per liter from Sigma Aldrich, while toluene can be purchased for \$82.60 per liter. Barring significant changes to supply lines, manufacturing processes, and/or demand, it would be difficult to implement an industrial-scale process with 2-MeTHF. D-Limonene is a notable exception. It is produced in higher volumes than the other chemicals of interest and is used as a cleaning additive (Sharma et al., 2017). However, it is not commonly employed as a reagent in laboratory settings, so quality control can be a challenge when investigating its properties. Additionally, although all of the solvents were selected because they were either less hazardous or more renewably produced than toluene, they are not hazard-free, as discussed in the Methods section. Several research groups are currently developing processes to synthesize biorenewable toluene, which could allow it to be used as sustainably as some of the potential alternatives that have similar hazard levels (Wijaya et al. 2016, Niziolek et al. 2016).

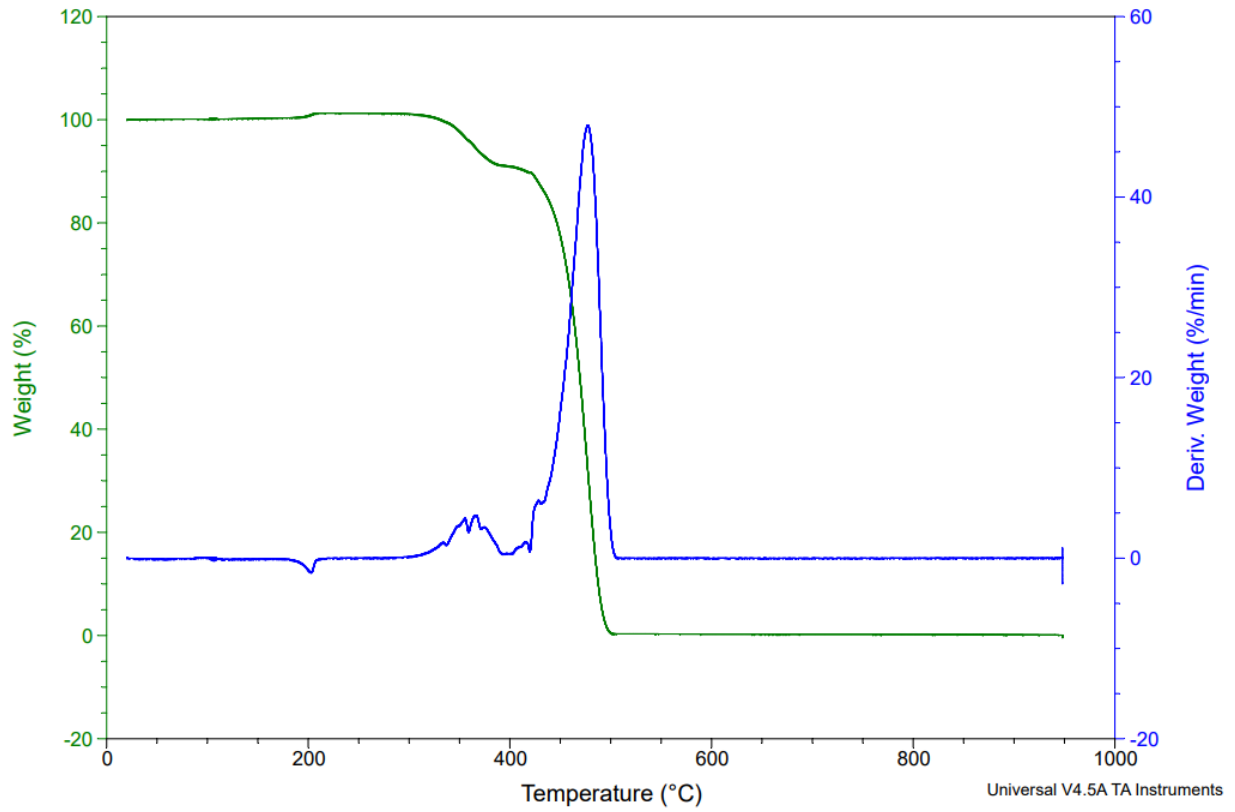
#### *Gasification & Pyrolysis of EVA*

We used thermogravimetric analysis to study how the EVA decomposes when heated. These experiments, under an inert atmosphere, can show the organic volatile components. Our testing indicates that under pyrolysis conditions no char is produced. Additionally, as shown in Figure 32 below, the decomposition range of EVA is between 350-500°C.



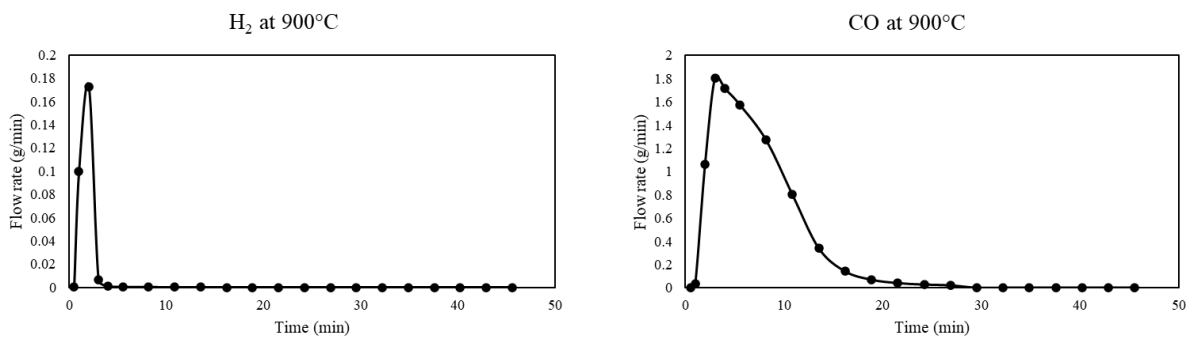
**Figure 32.** Thermogravimetric analysis curve for EVA under pyrolysis conditions.

Below is Figure 33, the derivative of the weight percentage overlaid with the weight percentage with respect to temperature. By overlaying the two curves, one can visualize how much percent weight is lost and the rate of this weight change. This indicates the presence of two distinct peaks of rapid decomposition, the second peak being significantly larger. The first peak is due to the deacetylation occurring. In other words, the first set of weight loss is due to losing acetic acid. The larger peak of decomposition rate is due to chain scission, meaning the main polymer thermally degrades—the C-C bonds are degrading.



**Figure 33.** Derivative plot overlaid with thermogravimetric analysis results.

As for the gasification experiments, as shown from Equation 1, the mass flow rates of the resulting gases can be found. Figure 34 indicate such results.



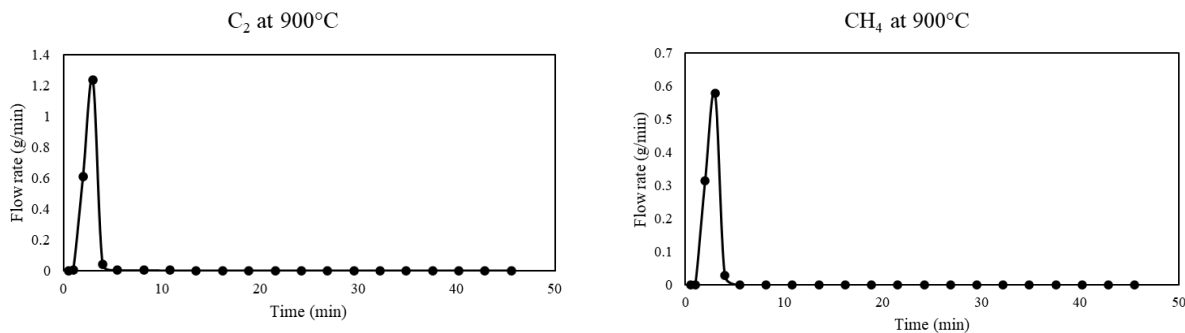


**Figure 34.** Syngas resultant gas flow rates at 900°C.

The plots above are the mass flow rates of H<sub>2</sub>, CO, CH<sub>4</sub>, and C<sub>2</sub>H<sub>x</sub> with respect to time at 900 °C. The evolution of these byproducts over time can be identified. When comparing the curves, it is interesting to note that after 5 minutes, only carbon monoxide is produced while there is no H<sub>2</sub>, CH<sub>4</sub>, or C<sub>2</sub>H<sub>x</sub>. Because of the high-temperature nature of this gasification, it is expected that CO forms in larger quantities, especially due to the oxygen-limited state of the experiments which promotes incomplete combustion. What is important to note here is the immense amount of CO produced relative to C<sub>2</sub>, CH<sub>4</sub>, and H<sub>2</sub> in our syngas. This is due to the fact that the gasification system was assisted with CO<sub>2</sub>: the carbons from the EVA and the CO<sub>2</sub> formed CO. This CO is partially oxidized and can be repurposed and used for other chemical applications such as fuel production and refining. Additionally, the finding is reconfirmed in the cumulative mass yields of the H<sub>2</sub>, CO, CH<sub>4</sub>, C<sub>2</sub>. Below is Table 3 showing the total mass yields.

**Table 3.** Total mass yields by species detected in the gasification experiments.

Species	H <sub>2</sub>	CO	CH <sub>4</sub>	C <sub>2</sub>
Mass Yield (g)	0.24	14.58	0.83	1.49

With the initial 10 gram sample of EVA used for gasification, the final mass yield is 17.14 grams of syngas. This is due to the fact the system was assisted with CO<sub>2</sub>. Below is Figure 35 which highlights the immense amount of CO relative to all other species in the syngas. It shows both the syngas yield and syngas energy.

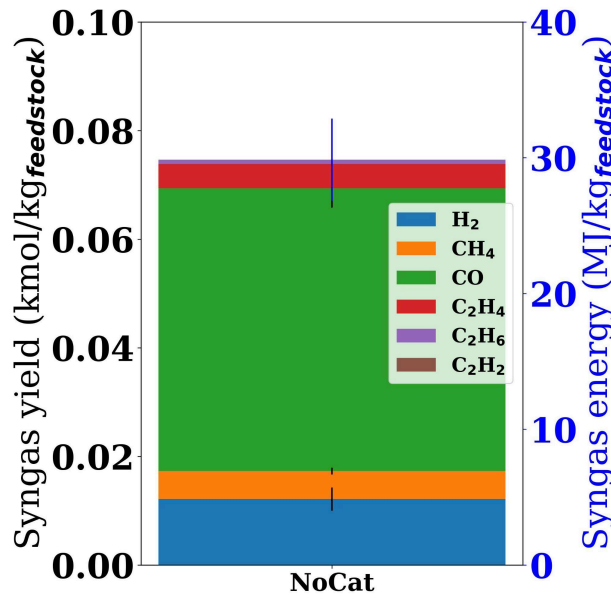


**Figure 35.** Syngas composition and energy resulting from gasification experiments.

Syngas energy is indicative of the calorific value, i.e. the energy released when a gas is burned. As expected with gasification, the syngas can be used for other purposes. In this situation, the total energy that can be reasonably expected to be released is 30 MJ/kg of EVA. The calorific value of EVA itself is 39.51 MJ/kg (Trivedi et al. 2023). Although the syngas energy is lower than the EVA, the syngas would provide an efficient burn without soot that can produce useful intermediates. The syngas can capture about 77% of the EVA calorific value. Burning of EVA itself would not be efficient and produce considerable soot. It is important to note that the gasification process itself also requires energy but the EVA syngas has considerable potential energy output.

When comparing to existing literature on the pyrolysis of EVA, Zeng et al. found that the pyrolysis gas was composed of 26.11% CO<sub>2</sub>, 22.12% CH<sub>4</sub>, and 8.43% H<sub>2</sub>, in terms of volumetric concentration, with the remainder being other hydrocarbons. As shown above, CO<sub>2</sub> was predominant followed by CO, CH<sub>4</sub>, C<sub>2</sub>H<sub>x</sub>, and H<sub>2</sub>. Our results follow existing literature with a large difference being the presence of CO. This is due to the differences in oxygen presence between gasification and pyrolysis. The literature performing gasification only analyzed the composition of a few oils and residues produced. Therefore, this EVA gasification helps advance the study of this topic in that it addresses the gap in syngas analysis.

## Conclusions and Future Works

### *Conclusions*

Although it was difficult to find a consistent metric to quantify a given solvent's effect on EVA, all solvents investigated in this study had a visible effect on the backsheet/wafer/EVA adhesion in solar panel fragments. At 70°C, panels treated with d-limonene and 2-MeTHF showed comparable mass loss to those treated with toluene, and Cyrene at 190°C exceeded the performance of toluene. While d-limonene and 2-MeTHF facilitated significant conformational change in the panels and reduced EVA/silicon adhesion, EGDA and Cyrene removed the backsheet without causing large amounts of EVA swelling, helping maintain the structural integrity of the silicon wafer. Both of these panel breakdown mechanisms could be advantageous, depending on the desired form of silicon recovery. As observed in previous solar recycling studies, EVA remained attached to silicon wafers post-treatment, indicating that thermal treatment may be necessary to completely remove EVA (Kang et al. 2012). Preliminary trials indicate that when EVA is gasified, the syngas can produce useful intermediates, namely the partially oxidized CO. Thus, further investigations into sustainable EVA thermal treatments should be conducted.

### *Contribution*

Overall, this research identified several promising paths towards reducing the environmental impact of the solar recycling process. Moving forward, research in this area would benefit from tests on unbroken panels, chemical composition analysis of post-treatment panels and solvents, and tests on other types of panels, such as CdTe thin films. Finally, it is important to consider the important role that environmental policy plays in the issue of solar waste. If solar recycling is to

become a widespread practice in the United States, a push for more stringent E-waste policies should be made.

### *Future Work*

For those solvents that caused dramatic conformational changes in the solar panel samples, it would be constructive to test them at lower temperatures, to see if the backsheet can be removed without causing the same degree of wafer fragmentation. Additional higher-temperature testing of certain solvents, such as ethyl oleate, might also allow for backsheet removal. As mentioned above, our experimental methods utilized magnetic stir bars which often collided with the solar panel fragments in solution; using a sonicator instead might prevent damages from the stir bar and allow for greater penetration of the solvent into the panel, aiding separation (Kim and Lee, 2012).

Completing solvent testing on an unbroken solar panel, rather than a glassless fragment, would be vital for ensuring the scalability of our results. In our preliminary tests with a full solar panel, we found that the five-hour timespan used for our other experiments did not result in significant changes to panel structure. With a glass front covering most of the EVA, the solvent could not penetrate fully into the central layers of the solar panel in the 5-hour timeframe. A days-long experiment has the potential to solve this problem, and as mentioned previously the use of a sonicator may speed this process up. Other pre-treatments, such as scoring the backsheet to allow solvent penetration to the semiconductor and encapsulant layers quicker, could be considered in future experiments as well. This would also allow for the execution of glass-on testing.

To determine more information about the effectiveness of chemical treatments than is provided through mass loss measurements, additional analytical testing on the recovered solvents

could be completed. Fourier transform infrared spectroscopy (FTIR) could be used to identify the presence of EVA or other panel fragments in the solvent, after chemical treatment. Ultimately, it is challenging to quantify “how well something fell apart,” but additional qualitative metrics such as FTIR or even UV-Vis absorbance spectroscopy could indicate the presence of dissolved EVA in the solvents, and provide relative information about the quantity. These methods could be used for both the EVA and solar panel sample trials. One quantitative treatment that could be used is scanning electron microscopy with energy dispersive X-ray spectroscopy (SEM-EDX) on the solar panel fragment itself, before and after chemical treatment, to compare the amounts of EVA present in the panel by identifying elemental presence.

In literature, thermal solar panel recycling techniques have been applied to remove both adhesive EVA layers and backsheet layers. Thermal removal eliminates chemical waste issues, but since many backsheet materials contain fluorinated compounds, backsheet pyrolysis can generate harmful gaseous byproducts such as hydrofluoric acid (Aryan et al., 2018; Fiandra et al., 2019). The gasification setup in this study was only applied to EVA, but it would be worthwhile to apply the treatment to panel backsheets as well. The chemical composition of the product gasses from the gasification-based thermal treatment could be compared to those from a pyrolysis-based thermal treatment to see if gasification can reduce the formation of harmful byproducts.

For consistency and convenience, all solar panels we used in this study were purchased new for the project. However, once a baseline has been established with new panels, testing any potential recycling process on aged panels is also vital for determining its efficacy. As panels age, EVA degrades due to exposure to UV radiation and intense weathering. As a result, its chemical properties and degree of cross-linking can change, changing its reaction to various

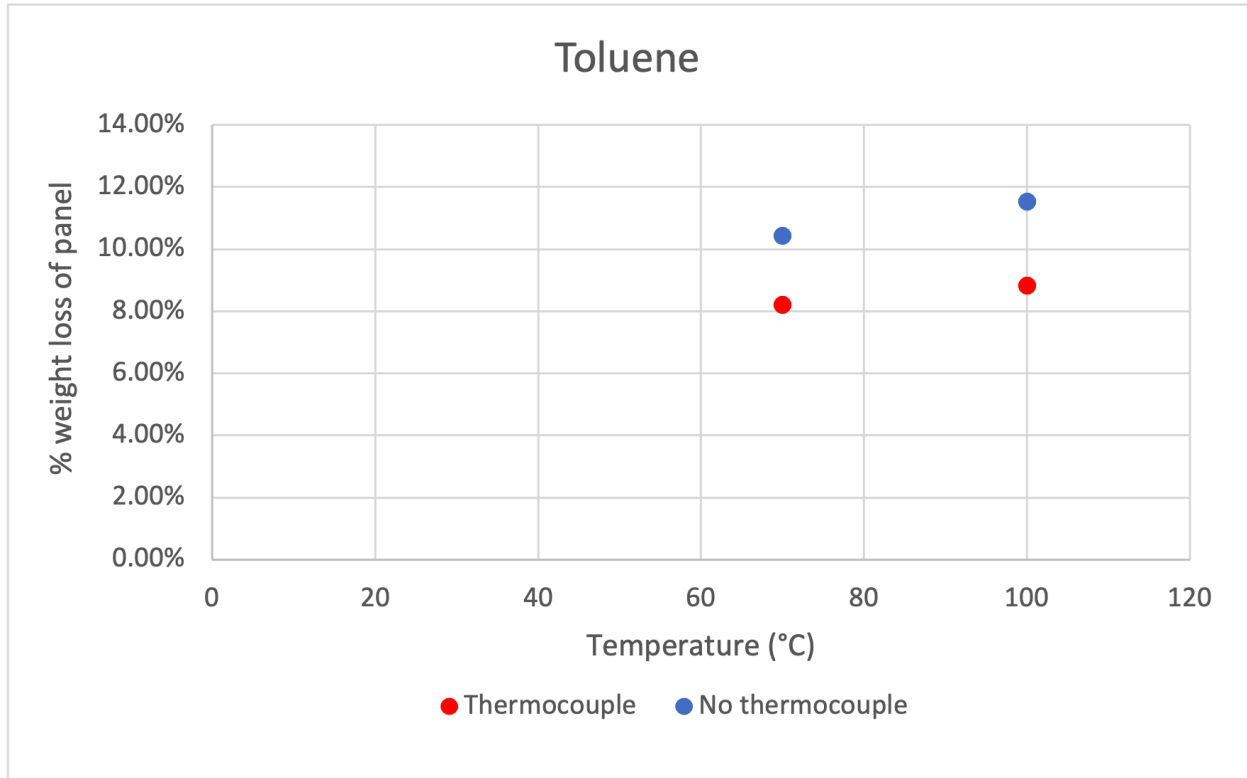
recycling treatments (Chowdhury et al., 2020). Finally, as discussed previously, we focused our study on crystalline silicon photovoltaics due to their prevalence, but it would be beneficial to test these methods on other types of panels. Thin-film CdTe photovoltaics also commonly use EVA encapsulants, but the differing mechanical and chemical properties of the semiconducting layer may result in different reactions to treatment (Aitola et al., 2022).

The waste from our process mainly consists of used solvents containing EVA. A significant portion of future work should include testing the reusability of our chosen solvents. This would involve determining the limit for how much EVA the solvent can contain and still be effective in the recycling process and ways of separating EVA from the solvent. Separation strategies for recycling and reusing solvents in the literature include centrifugation, membrane processes, and distillation (Aboagye et al., 2021). For small pieces of EVA that are not dissolved, centrifugation would likely be effective at removing these suspended particles. Membrane separations based on the size difference between the EVA polymer and the solvent molecule should also be investigated. Distillation is a high-energy method that may not be cost-effective, but it would be able to separate our chosen solvents (highest boiling point of 227 °C) from EVA (decomposition above 350 °C as shown by our TGA analysis). Once the solvent becomes too impure to be reused, or if the recycling process would not be beneficial from a lifecycle perspective, we will consider solvent disposal methods. This generally involves incineration.

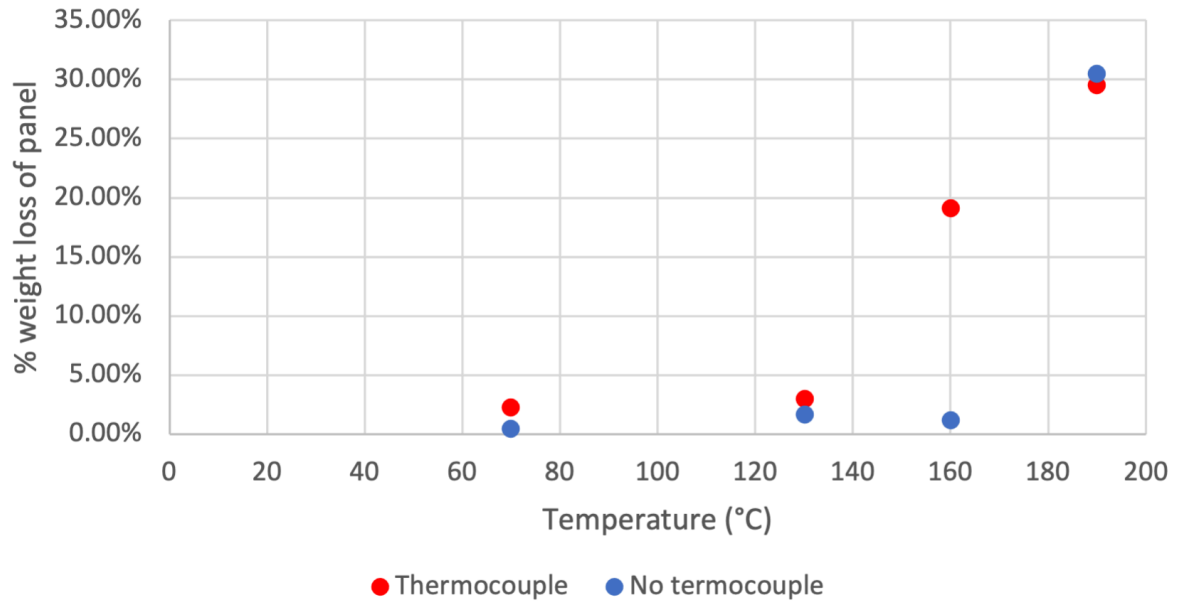
Future work will also include developing a process for reusing the recovered silicon cell fragments. After the solvent treatment step, these fragments would also contain leftover solvent, which as seen in our work can be difficult to remove. The gasification process, if performed on these fragments, could remedy this issue and remove remaining EVA, leaving behind clean silicon pieces that are more readily reused.

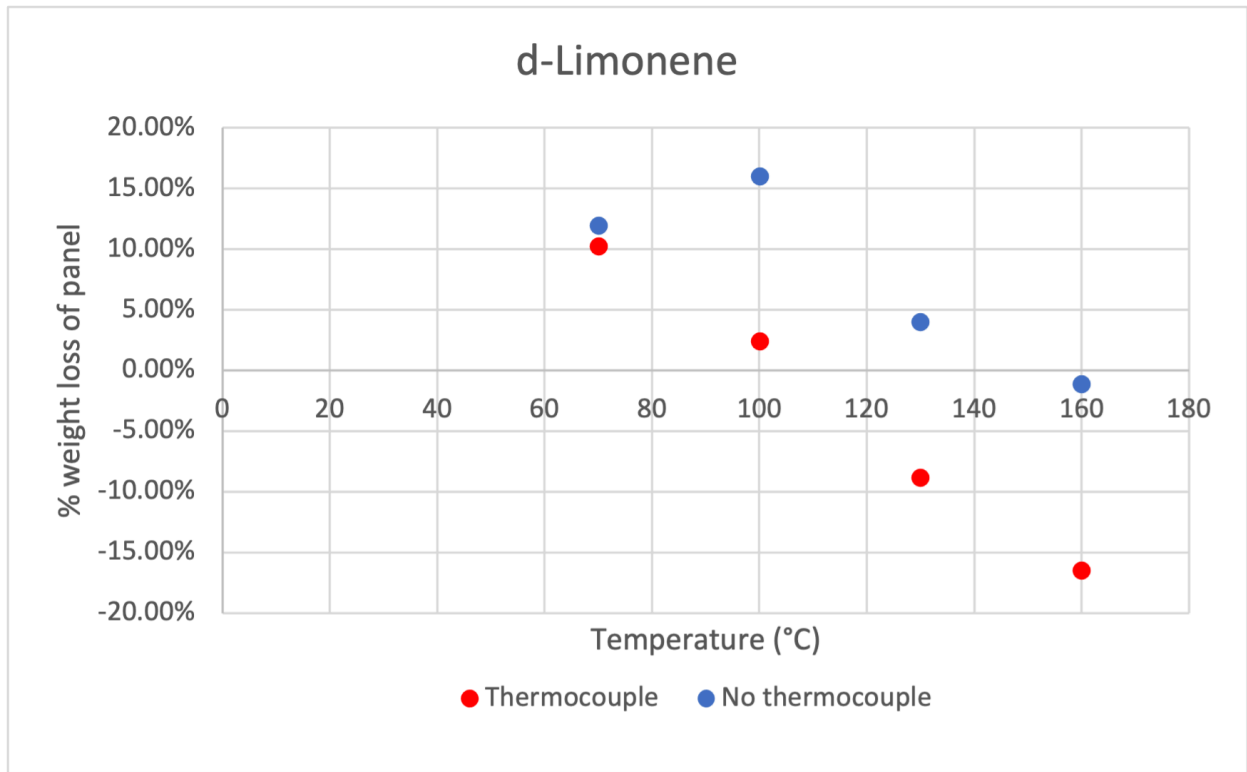
## Appendices

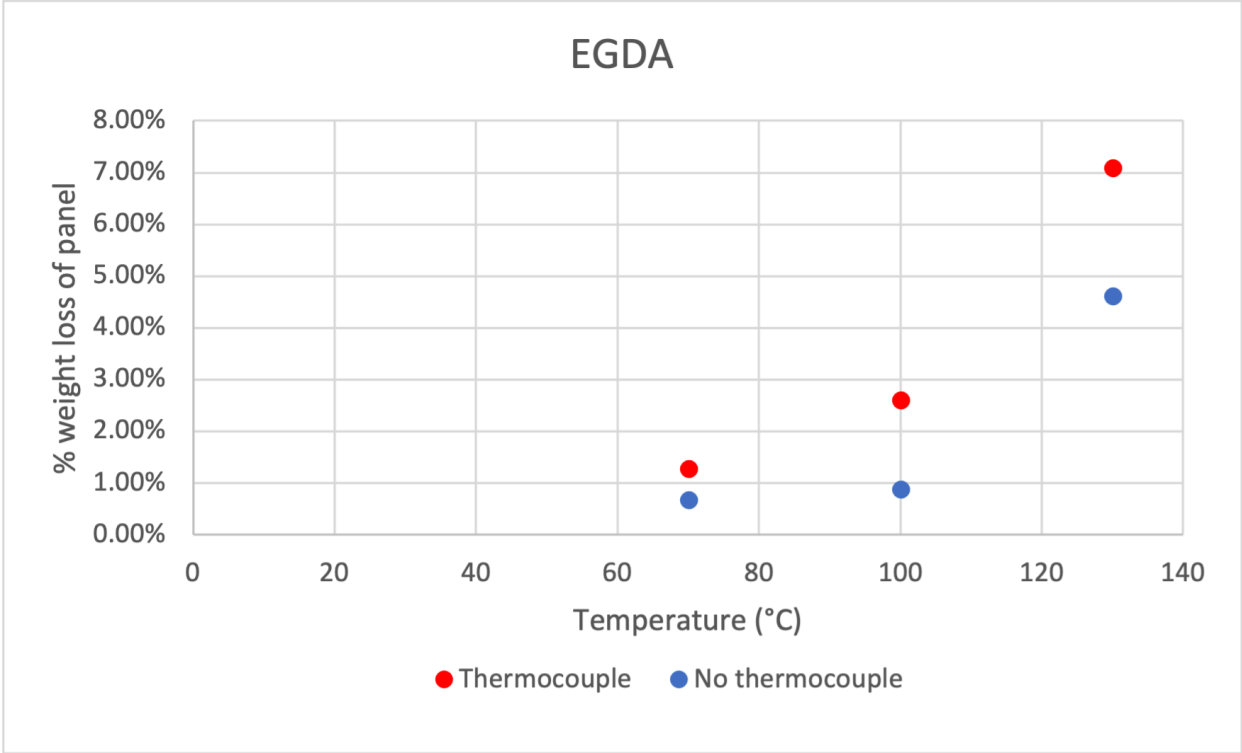
### *Appendix A: Impact of thermocouple presence on sample mass loss*



# Cyrene







## References

- Abdo, D. M., El-Shazly, A. N., & Medici, F. (2023). Recovery of Valuable Materials from End-of-Life Photovoltaic Solar Panels. *Materials*, *16*(7), 2840.  
<https://doi.org/10.3390/ma16072840>
- Aboagye, E. A., Chea, J. D., & Yenkie, K. M. (2021). Systems level roadmap for solvent recovery and reuse in industries. *iScience*, *24*(10), 103114.  
<https://doi.org/10.1016/j.isci.2021.103114>
- Abott, S. (2024). *HSP Basics*.  
<https://www.stevenabbott.co.uk/practical-solubility/hsp-basics.php>
- Ahmed, I. I., Nipattummakul, N., & Gupta, A. K. (2011). Characteristics of syngas from co-gasification of polyethylene and woodchips. *Applied Energy*, *88*(1), 165–174.  
<https://doi.org/10.1016/j.apenergy.2010.07.007>
- Aitola, K., Gava Sonai, G., Markkanen, M., Jaqueline Kaschuk, J., Hou, X., Miettunen, K., & Lund, P. D. (2022). Encapsulation of commercial and emerging solar cells with focus on perovskite solar cells. *Solar Energy*, *237*, 264–283.  
<https://doi.org/10.1016/j.solener.2022.03.060>
- Aman, M. M., Solangi, K. H., Hossain, M. S., Badarudin, A., Jasmon, G. B., Mokhlis, H., Bakar, A. H. A., & Kazi, S. N. (2015). A review of Safety, Health and Environmental (SHE) issues of solar energy system. *Renewable and Sustainable Energy Reviews*, *41*, 1190–1204. <https://doi.org/10.1016/j.rser.2014.08.086>
- Aryan, V., Font-Brucart, M., & Maga, D. (2018). A comparative life cycle assessment of end-of-life treatment pathways for photovoltaic backsheets. *Progress in Photovoltaics: Research and Applications*, *26*(7), 443–459. <https://doi.org/10.1002/pip.3003>

- Aycock, D. F. (2007). Solvent Applications of 2-Methyltetrahydrofuran in Organometallic and Biphasic Reactions. *Organic Process Research & Development*, 11(1), 156–159. <https://doi.org/10.1021/op060155c>
- Azeumo, M. F., Germana, C., Ippolito, N. M., Franco, M., Luigi, P., & Settimio, S. (2019). Photovoltaic module recycling, a physical and a chemical recovery process. *Solar Energy Materials and Solar Cells*, 193, 314–319. <https://doi.org/10.1016/j.solmat.2019.01.035>
- Beyer, M. (2022, February 15). *New PV module recycling tech from France*. Pv Magazine International. <https://www.pv-magazine.com/2022/02/15/new-pv-module-recycling-tech-from-france/>
- Bomgardner, M. (2018). How First Solar recycles its CdTe panels. *C&EN Global Enterprise*, 96(15), 40–40. <https://doi.org/10.1021/cen-09615-cover2>
- Bookstaff, R. C., PaiBir, S., Bharaj, S. S., Kelm, G. R., Kulick, R. M., Balm, T. K., & Murray, J. V. (2003). The safety of the use of ethyl oleate in food is supported by metabolism data in rats and clinical safety data in humans. *Regulatory Toxicology and Pharmacology*, 37(1), 133–148. [https://doi.org/10.1016/S0273-2300\(02\)00043-0](https://doi.org/10.1016/S0273-2300(02)00043-0)
- Boyd, E., Chaffin, B. C., Dorkenoo, K., Jackson, G., Harrington, L., N'Guetta, A., Johansson, E. L., Nordlander, L., Paolo De Rosa, S., Raju, E., Scown, M., Soo, J., & Stuart-Smith, R. (2021). Loss and damage from climate change: A new climate justice agenda. *One Earth*, 4(10), 1365–1370. <https://doi.org/10.1016/j.oneear.2021.09.015>
- Cannon, C. (2020). Examining Rural Environmental Injustice: An Analysis of Ruralness, Class, Race, and Gender On the Presence of Landfills Across the United States. *Journal of Rural and Community Development*, 15(1), Article 1.

<https://journals.brandonu.ca/jrcd/article/view/1737>

Chee, A. K.-W. (2023). On current technology for light absorber materials used in highly efficient industrial solar cells. *Renewable and Sustainable Energy Reviews*, 173, 113027. <https://doi.org/10.1016/j.rser.2022.113027>

Chowdhury, Md. S., Rahman, K. S., Chowdhury, T., Nuthammachot, N., Techato, K., Akhtaruzzaman, Md., Tiong, S. K., Sopian, K., & Amin, N. (2020). An overview of solar photovoltaic panels' end-of-life material recycling. *Energy Strategy Reviews*, 27, 100431. <https://doi.org/10.1016/j.esr.2019.100431>

Citarella, A., Amenta, A., Passarella, D., & Micale, N. (2022). Cyrene: A Green Solvent for the Synthesis of Bioactive Molecules and Functional Biomaterials. *International Journal of Molecular Sciences*, 23(24), 15960. <https://doi.org/10.3390/ijms232415960>

Contreras-Lisperguer, R., Muñoz-Cerón, E., Aguilera, J., & Casa, J. de la. (2017). Cradle-to-cradle approach in the life cycle of silicon solar photovoltaic panels. *Journal of Cleaner Production*, 168, 51–59. <https://doi.org/10.1016/j.jclepro.2017.08.206>

Council of State Governments. (2022, October 18). *Research Memorandum: Solar Panel Recycling - The Council of State Governments*. <https://www.csg.org/2022/10/18/research-memorandum/>

Dambhare, M. V., Butey, B., & Moharil, S. V. (2021). Solar photovoltaic technology: A review of different types of solar cells and its future trends. *Journal of Physics: Conference Series*, 1913(1), 012053. <https://doi.org/10.1088/1742-6596/1913/1/012053>

Date, A. A., Srivastava, D., Nagarsenker, M. S., Mulherkar, R., Panicker, L., Aswal, V., Hassan, P. A., Steiniger, F., Thamm, J., & Fahr, A. (2011). Lecithin-based novel cationic nanocarriers (LeciPlex) I: Fabrication, characterization and evaluation.

*Nanomedicine*, 6(8), 1309–1325. <https://doi.org/10.2217/nmm.11.38>

Díaz de los Ríos, M., & Ramos, E. (2020). Determination of the Hansen solubility parameters and the Hansen sphere radius with the aid of the solver add-in of Microsoft Excel. *SN Applied Sciences*, 2. <https://doi.org/10.1007/s42452-020-2512-y>

Dintcheva, N. T., Morici, E., & Colletti, C. (2023). Encapsulant Materials and Their Adoption in Photovoltaic Modules: A Brief Review. *Sustainability*, 15(12), 9453. <https://doi.org/10.3390/su15129453>

*D-Limonene CASRN 5989-27-5*. (1993). [Reports & Assessments]. IRIS | US EPA, ORD. [https://iris.epa.gov/ChemicalLanding/&substance\\_nmbr=682](https://iris.epa.gov/ChemicalLanding/&substance_nmbr=682)

Dobra, T., Vollprecht, D., & Pomberger, R. (2022). Thermal delamination of end-of-life crystalline silicon photovoltaic modules. *Waste Management & Research: The Journal for a Sustainable Circular Economy*, 40(1), 96–103. <https://doi.org/10.1177/0734242X211038184>

Doi, T., Tsuda, I., Unagida, H., Murata, A., Sakuta, K., & Kurokawa, K. (2001). Experimental study on PV module recycling with organic solvent method. *Solar Energy Materials and Solar Cells*, 67(1–4), 397–403. [https://doi.org/10.1016/S0927-0248\(00\)00308-1](https://doi.org/10.1016/S0927-0248(00)00308-1)

El Amrani, A., Mahrane, A., Moussa, F. Y., & Boukennous, Y. (2007). Solar Module Fabrication. *International Journal of Photoenergy*, 2007, e27610. <https://doi.org/10.1155/2007/27610>

*End-of-life management: Solar Photovoltaic Panels*. (2016, June 1). IRENA | International Renewable Energy Agency. <https://www.irena.org/publications/2016/Jun/End-of-life-management-Solar-Photovoltaic>

## c-Panels

*Ethyl Oleate*. (2023). NIST Chemistry WebBook, SRD 69.

<https://webbook.nist.gov/cgi/inchi?ID=C111626&Mask=4>

*Ethylene glycol diacetate*. (n.d.). PubChem. Retrieved March 28, 2024, from

<https://pubchem.ncbi.nlm.nih.gov/compound/8121>

Fiandra, V., Sannino, L., Andreozzi, C., Corcelli, F., & Graditi, G. (2019). Silicon photovoltaic modules at end-of-life: Removal of polymeric layers and separation of materials. *Waste Management*, 87, 97–107.

<https://doi.org/10.1016/j.wasman.2019.02.004>

First Solar. (2017). *Sustainability Documents*. First Solar.

<https://www.firstsolar.com:443/Resources/Sustainability-Documents>

Fowles, J., Boatman, R., Bootman, J., Lewis, C., Morgott, D., Rushton, E., van Rooij, J., & Banton, M. (2013). A review of the toxicological and environmental hazards and risks of tetrahydrofuran. *Critical Reviews in Toxicology*, 43(10), 811–828.

<https://doi.org/10.3109/10408444.2013.836155>

Geretschläger, K. J., Wallner, G. M., & Fischer, J. (2016). Structure and basic properties of photovoltaic module backsheets. *Solar Energy Materials and Solar Cells*, 144, 451–456. <https://doi.org/10.1016/j.solmat.2015.09.060>

Giacchetta, G., Leporini, M., & Marchetti, B. (2013). Evaluation of the environmental benefits of new high value process for the management of the end of life of thin film photovoltaic modules. *Journal of Cleaner Production*, 51, 214–224.

<https://doi.org/10.1016/j.jclepro.2013.01.022>

Granata, G., Pagnanelli, F., Moscardini, E., Havlik, T., & Toro, L. (2014). Recycling of

photovoltaic panels by physical operations. *Solar Energy Materials and Solar Cells*, 123, 239–248. <https://doi.org/10.1016/j.solmat.2014.01.012>

*Heat Values of Various Fuels*. (n.d.). World Nuclear Association.

<https://world-nuclear.org/information-library/facts-and-figures/heat-values-of-various-fuels.aspx>

Held, M., & Ilg, R. (2011). Update of environmental indicators and energy payback time of CdTe PV systems in Europe. *Progress in Photovoltaics: Research and Applications*, 19(5), 614–626. <https://doi.org/10.1002/pip.1068>

Hidayanti, F. (2020). *The Effect of Monocrystalline and Polycrystalline Material Structure on Solar Cell Performance*.

Hou, G., Sun, H., Jiang, Z., Pan, Z., Wang, Y., Zhang, X., Zhao, Y., & Yao, Q. (2016). Life cycle assessment of grid-connected photovoltaic power generation from crystalline silicon solar modules in China. *Applied Energy*, 164, 882–890.

<https://doi.org/10.1016/j.apenergy.2015.11.023>

Huang, W.-H., Shin, W. J., Wang, L., Sun, W.-C., & Tao, M. (2017). Strategy and technology to recycle wafer-silicon solar modules. *Solar Energy*, 144, 22–31.

<https://doi.org/10.1016/j.solener.2017.01.001>

Hurdle, J. (2023, February 28). *As Millions of Solar Panels Age Out, Recyclers Hope to Cash In*. Yale E360. <https://e360.yale.edu/features/solar-energy-panels-recycling>

Hutchinson, D. (2023, October 19). *States Weigh Making Industry Pay Millions For Solar Panel Waste*. Bloomberg Law News.

<https://news.bloomberglaw.com/environment-and-energy/states-weigh-making-industry-pay-millions-for-solar-panel-waste>

*Hydrogen Fluoride (Hydrofluoric Acid)*. (2016). US EPA | National Service Center for Environmental Publications.

<https://nepis.epa.gov/Exe/ZyNET.exe/P1014A6O.TXT?ZyActionD=ZyDocument&Client=EPA&Index=2016+Thru+2020&Docs=&Query=&Time=&EndTime=&SearchMethod=1&TocRestrict=n&Toc=&TocEntry=&QField=&QFieldYear=&QFieldMonth=&QFieldDay=&IntQFieldOp=0&ExtQFieldOp=0&XmlQuery=&File=D%3A%5Czyfiles%5CIndex%20Data%5C16thru20%5CTxt%5C00000028%5CP1014A6O.txt&User=ANONYMOUS&Password=anonymous&SortMethod=h%7C-&MaximumDocuments=1&FuzzyDegree=0&ImageQuality=r75g8/r75g8/x150y150g16/i425&Display=hpfr&DefSeekPage=x&SearchBack=ZyActionL&Back=ZyActionS&BackDesc=Results%20page&MaximumPages=1&ZyEntry=1&SeekPage=x&ZyPURL>

Isherwood, P. J. M. (2022). Reshaping the Module: The Path to Comprehensive Photovoltaic Panel Recycling. *Sustainability*, 14(3), Article 3. <https://doi.org/10.3390/su14031676>

Jiang, L., Cui, S., Sun, P., Wang, Y., & Yang, C. (2020). Comparison of Monocrystalline and Polycrystalline Solar Modules. *2020 IEEE 5th Information Technology and Mechatronics Engineering Conference (ITOEC)*, 341–344. <https://doi.org/10.1109/ITOEC49072.2020.9141722>

Kang, S., Yoo, S., Lee, J., Boo, B., & Ryu, H. (2012). Experimental investigations for recycling of silicon and glass from waste photovoltaic modules. *Renewable Energy*, 47, 152–159. <https://doi.org/10.1016/j.renene.2012.04.030>

Kim, Y., & Lee, J. (2012). Dissolution of ethylene vinyl acetate in crystalline silicon PV modules using ultrasonic irradiation and organic solvent. *Solar Energy Materials and Solar Cells*, 98, 317–322. <https://doi.org/10.1016/j.solmat.2011.11.022>

- Koller, G., Fischer, U., & Hungerbühler, K. (2000). Assessing Safety, Health, and Environmental Impact Early during Process Development. *Industrial & Engineering Chemistry Research*, 39(4), 960–972. <https://doi.org/10.1021/ie990669j>
- Latunussa, C. E. L., Ardente, F., Blengini, G. A., & Mancini, L. (2016). Life Cycle Assessment of an innovative recycling process for crystalline silicon photovoltaic panels. *Solar Energy Materials and Solar Cells*, 156, 101–111. <https://doi.org/10.1016/j.solmat.2016.03.020>
- Limonene, (+)-. (2024). PubChem. <https://pubchem.ncbi.nlm.nih.gov/compound/440917>
- Maalouf, A., Okoroafor, T., Jehl, Z., Babu, V., & Resalati, S. (2023). A comprehensive review on life cycle assessment of commercial and emerging thin-film solar cell systems. *Renewable and Sustainable Energy Reviews*, 186, 113652. <https://doi.org/10.1016/j.rser.2023.113652>
- Maani, T., Celik, I., Heben, M. J., Ellingson, R. J., & Apul, D. (2020). Environmental impacts of recycling crystalline silicon (c-Si) and cadmium telluride (CDTE) solar panels. *Science of The Total Environment*, 735, 138827. <https://doi.org/10.1016/j.scitotenv.2020.138827>
- Marchetti, B., Corvaro, F., Giacchetta, G., Polonara, F., Cocci Grifoni, R., & Leporini, M. (2018). Double Green Process: A low environmental impact method for recycling of CdTe, a-Si and CIS/CIGS thin-film photovoltaic modules. *International Journal of Sustainable Engineering*, 11(3), 173–185. <https://doi.org/10.1080/19397038.2018.1424963>
- Mavukwana, A., Burra, K. G., Sempuga, C., Castaldi, M., & Gupta, A. K. (2023). Effect of gypsum waste inclusion on syngas production during CO<sub>2</sub>-assisted gasification of waste

- tires. *Waste Management*, 171, 375–381. <https://doi.org/10.1016/j.wasman.2023.09.022>
- Medical Management Guidelines for Toluene*. (2014). ASDR Toxic Substances Portal. <https://wwwn.cdc.gov/TSP/MMG/MMGDetails.aspx?mmgid=157&toxid=29>
- Mencer, H. J., & Gomzi, Z. (1994). Swelling kinetics of polymer-solvent systems. *European Polymer Journal*, 30(1), 33–36. [https://doi.org/10.1016/0014-3057\(94\)90229-1](https://doi.org/10.1016/0014-3057(94)90229-1)
- Min, R., Li, K., Wang, D., Xiao, W., Liu, C., Wang, Z., & Bian, S. (2023). A novel method for layer separation of photovoltaic modules by using green reagent EGDA. *Solar Energy*, 253, 117–126. <https://doi.org/10.1016/j.solener.2023.02.024>
- Mitra, S., Chakraborty, A. J., Tareq, A. M., Emran, T. B., Nainu, F., Khusro, A., Idris, A. M., Khandaker, M. U., Osman, H., Alhumaydhi, F. A., & Simal-Gandara, J. (2022). Impact of heavy metals on the environment and human health: Novel therapeutic insights to counter the toxicity. *Journal of King Saud University - Science*, 34(3), 101865. <https://doi.org/10.1016/j.jksus.2022.101865>
- Moutinho, H., To, B., Sulas-Kern, D., Jiang, C.-S., Al-Jassim, M., & Johnston, S. (2020). Advances in Coring Procedures of Silicon Photovoltaic Modules. *2020 47th IEEE Photovoltaic Specialists Conference (PVSC)*, 1449–1453. <https://doi.org/10.1109/PVSC45281.2020.9300408>
- Nain, P., & Kumar, A. (2020). Initial metal contents and leaching rate constants of metals leached from end-of-life solar photovoltaic waste: An integrative literature review and analysis. *Renewable and Sustainable Energy Reviews*, 119, 109592. <https://doi.org/10.1016/j.rser.2019.109592>
- Niziolek, A. M., Onel, O., Guzman, Y. A., & Floudas, C. A. (2016). Biomass-Based Production of Benzene, Toluene, and Xylenes via Methanol: Process Synthesis and

Deterministic Global Optimization. *Energy & Fuels*, 30(6), 4970–4998.

<https://doi.org/10.1021/acs.energyfuels.6b00619>

Nover, J., Zapf-Gottwick, R., Feifel, C., Koch, M., Metzger, J. W., & Werner, J. H. (2017).

Long-term leaching of photovoltaic modules. *Japanese Journal of Applied Physics*, 56(8S2), 08MD02. <https://doi.org/10.7567/JJAP.56.08MD02>

Ogunseitan, O. A. (2023). The Environmental Justice Agenda for E-Waste Management.

*Environment: Science and Policy for Sustainable Development*, 65(2), 15–25.

<https://doi.org/10.1080/00139157.2023.2167457>

Padoan, F. C. S. M., Altimari, P., & Pagnanelli, F. (2019). Recycling of end of life

photovoltaic panels: A chemical prospective on process development. *Solar Energy*, 177, 746–761. <https://doi.org/10.1016/j.solener.2018.12.003>

Papež, N., Dallaev, R., Țălu, Ș., & Kaštyl, J. (2021). Overview of the Current State of

Gallium Arsenide-Based Solar Cells. *Materials*, 14(11), 3075.

<https://doi.org/10.3390/ma14113075>

Park, J., Kim, W., Cho, N., Lee, H., & Park, N. (2016). An eco-friendly method for

reclaimed silicon wafers from a photovoltaic module: From separation to cell fabrication. *Green Chemistry*, 18(6), 1706–1714. <https://doi.org/10.1039/C5GC01819F>

Park, J., & Park, N. (2014). Wet etching processes for recycling crystalline silicon solar cells

from end-of-life photovoltaic modules. *RSC Adv.*, 4(66), 34823–34829.

<https://doi.org/10.1039/C4RA03895A>

Policella, M., Wang, Z., Burra, Kiran. G., & Gupta, A. K. (2019). Characteristics of syngas

from pyrolysis and CO<sub>2</sub>-assisted gasification of waste tires. *Applied Energy*, 254,

113678. <https://doi.org/10.1016/j.apenergy.2019.113678>

Qin, B., Lin, M., Zhang, X., Xu, Z., & Ruan, J. (2021). Recovering Polyethylene Glycol Terephthalate and Ethylene-Vinyl Acetate Copolymer in Waste Solar Cells via a Novel Vacuum-Gasification-Condensation Process. *ACS ES&T Engineering*, *1*(3), 357–362. <https://doi.org/10.1021/acsestengg.0c00091>

Seo, B., Kim, J. Y., & Chung, J. (2021). Overview of global status and challenges for end-of-life crystalline silicon photovoltaic panels: A focus on environmental impacts. *Waste Management*, *128*, 45–54. <https://doi.org/10.1016/j.wasman.2021.04.045>

Sharma, K., Mahato, N., Cho, M. H., & Lee, Y. R. (2017). Converting citrus wastes into value-added products: Economic and environmentally friendly approaches. *Nutrition*, *34*, 29–46. <https://doi.org/10.1016/j.nut.2016.09.006>

Sherwood, J., De Bruyn, M., Constantinou, A., Moity, L., McElroy, C. R., Farmer, T. J., Duncan, T., Raverty, W., Hunt, A. J., & Clark, J. H. (2014). Dihydrolevoglucosenone (Cyrene) as a bio-based alternative for dipolar aprotic solvents. *Chem. Commun.*, *50*(68), 9650–9652. <https://doi.org/10.1039/C4CC04133J>

Sicaire, A.-G., Vian, M., Filly, A., Li, Y., Bily, A., & Chemat, F. (2014). 2-Methyltetrahydrofuran: Main Properties, Production Processes, and Application in Extraction of Natural Products. In *Alternative Solvents for Natural Products Extraction* (pp. 253–268). [https://doi.org/10.1007/978-3-662-43628-8\\_12](https://doi.org/10.1007/978-3-662-43628-8_12)

Skomedal, A., & Deceglie, M. G. (2020). Combined Estimation of Degradation and Soiling Losses in Photovoltaic Systems. *IEEE Journal of Photovoltaics*, *10*(6), 1788–1796. <https://doi.org/10.1109/JPHOTOV.2020.3018219>

Snead, R. (2021, February 24). *Washington State Tackles Solar Panel Waste, the Dirty Side*

of *Clean Tech*. Environmental and Energy Study Institute.

<https://www.eesi.org/articles/view/washington-state-tackles-solar-panel-waste-the-dirty-side-of-clean-tech>

*Standard Test Methods for Proximate Analysis of Coal and Coke by Macro*

*Thermogravimetric Analysis*. (2023). ASTM International.

<https://compass.astm.org/document/?contentCode=ASTM%7CD7582-15%7Cen-US&proxycl=https%3A%2F%2Fsecure.astm.org&fromLogin=true>

Tabassum, S., Rahman, T., Islam, A. U., Rahman, S., Dipta, D. R., Roy, S., Mohammad, N.,

Nawar, N., & Hossain, E. (2021). Solar Energy in the United States: Development, Challenges and Future Prospects. *Energies*, *14*(23), Article 23.

<https://doi.org/10.3390/en14238142>

Tao, M., Fthenakis, V., Ebin, B., Steenari, B., Butler, E., Sinha, P., Corkish, R., Wambach,

K., & Simon, E. S. (2020). Major challenges and opportunities in silicon solar module recycling. *Progress in Photovoltaics: Research and Applications*, *28*(10), 1077–1088.

<https://doi.org/10.1002/pip.3316>

*Tetrahydrofuran*. (2015). American Chemical Society.

<https://www.acs.org/molecule-of-the-week/archive/t/tetrahydrofuran.html>

*Toluene*. (2024). PubChem. <https://pubchem.ncbi.nlm.nih.gov/compound/1140>

U.S. Dept of Energy Solar Energy Technologies Office. (2022). *Solar Energy Technologies*

*Office Photovoltaics End-of-Life Action Plan*.

[https://www.energy.gov/sites/default/files/2022-03/Solar-Energy-Technologies-Office-PV-End-of-Life-Action-Plan\\_0.pdf](https://www.energy.gov/sites/default/files/2022-03/Solar-Energy-Technologies-Office-PV-End-of-Life-Action-Plan_0.pdf)

US EPA National Center for Environmental Assessment. (2005). *Toluene*; CASRN 108-88-3

[Integrated Risk Information System Chemical Assessment Summary].

[https://iris.epa.gov/static/pdfs/0118\\_summary.pdf](https://iris.epa.gov/static/pdfs/0118_summary.pdf)

US EPA, O. (2023, October 3). *Improving Recycling and Management of Renewable Energy Wastes: Universal Waste Regulations for Solar Panels and Lithium Batteries* [Reports and Assessments].

<https://www.epa.gov/hw/improving-recycling-and-management-renewable-energy-wastes-universal-waste-regulations-solar>

Van den Broeck, K., Van Hoornick, N., Van Hoeymissen, J., de Boer, R., Giesen, A., & Wilms, D. (2003). Sustainable treatment of HF wastewaters from semiconductor industry with a fluidized bed reactor. *IEEE Transactions on Semiconductor Manufacturing*, 16(3), 423–428. <https://doi.org/10.1109/TSM.2003.815624>

*Water*. (2024). PubChem. <https://pubchem.ncbi.nlm.nih.gov/compound/962>

Wijaya, Y. P., Kristianto, I., Lee, H., & Jae, J. (2016). Production of renewable toluene from biomass-derived furans via Diels-Alder and dehydration reactions: A comparative study of Lewis acid catalysts. *Fuel*, 182, 588–596. <https://doi.org/10.1016/j.fuel.2016.06.010>

Xu, Y., Xue, X., Dong, L., Nai, C., Liu, Y., & Huang, Q. (2018). Long-term dynamics of leachate production, leakage from hazardous waste landfill sites and the impact on groundwater quality and human health. *Waste Management*, 82, 156–166.

<https://doi.org/10.1016/j.wasman.2018.10.009>

Zeng, D.-W., Born, M., & Wambach, K. (2004). Pyrolysis of EVA and its application in recycling of photovoltaic modules. *Journal of Environmental Sciences (China)*, 16(6), 889–893.